Russian Chemical Reviews **79** (7) 611 – 634 (2010) © 2010 Russian Academy of Sciences and Turpion Ltd

DOI 10.1070/RC2010v079n07ABEH004141

Tungsten carbides and nitrides and ternary systems based on them: the electronic structure, chemical bonding and properties

D V Suetin, I R Shein, A L Ivanovskii

Contents

I.	Introduction	611
II.	Tungsten carbides	612
III.	Tungsten nitrides	617
IV.	Ternary systems based on tungsten carbides and nitrides	620
V.	Conclusion	631

Abstract. The review is concerned with analysis of the results of modern *ab initio* studies on the electronic structure, the nature of chemical bonding and some physicochemical properties of tungsten carbides and nitrides (W_2C, WC, W_2N, WN, WN_2, WN_3) as well as ternary compounds and solid solutions based on them, *viz*., carbonitrides ($WC_{1-x}N_x$), aluminocarbides ($W_xAl_yC_z$), double carbides and nitrides with perovskite structures (M_3WC, W_3MC and W_3MN, where M are d-metals), η-carbides (M_3W_3C and M_6W_6C), *etc*. The results of studies on the structures, phase stabilities, elastic and magnetic properties of tungsten-containing systems and the corresponding predictions are discussed. The bibliography includes 186 references.

I. Introduction

Transition (3d – 5d) metal carbides and nitrides exhibit various combinations of interesting physicochemical properties (high strength and hardness, radiation stability, chemical inertness, extremal thermomechanical parameters) and unusual electrophysical, catalytic and magnetic characteristics.[1–9] This is due to peculiar features of the electronic structure and a complex system of interatomic bonds in these compounds[10–12] and predetermines a wide use of such systems in the design and production of various multifunctional materials.[1–12]

In addition to the binary carbides and nitrides of d-metals, there is a large number of multicomponent compounds and solid solutions based on them, *e.g*., carbonitrides, oxycarbides, oxycarbonitrides, hydridocarbides, hydridonitrides and various composites and ceramic materials. Recently, studies on the design of novel nanomaterials (in the form of nanopowders, nanostructured films, alloys, ceramics, composites, *etc*.) based on carbides and nitrides of d-metals as well as on the synthesis, investigations and simulation of the properties of carbides and nitrides in the form of molecular clusters, nanocrystallites, nanospheres, nanofilaments, nanowires, nanotunes, *etc*., have been carried out.[12–31]

Among the d-metal carbides and nitrides mentioned above, considerable attention of researchers is attracted to the phases that are formed in the W – C and W – N systems, to their solid solutions and to related ternary tungsten-containing phases.

On the one hand, this is due to attractive physicochemical properties of these systems. For instance, tungsten monocarbide (WC) is characterized by a small thermal expansion coefficient and high hardness, which are retained in a wide temperature interval.[32,33] At present, WC is widely used for production of wear-resistant tool alloys and various coatings.[33] Studies on fabrication of WC nanopowders, nanofilaments, nanotubes and nanocomposites are carried out.[34–42] Tungsten mononitride possesses a high hardness and good electrical conductivity[7,8] and is considered as a promising material for manufacturing of ohmic contacts for microelectronics.

On the other side, increased recent interest in tungsten carbides and nitrides is due to the following reasons. It has been assumed for long that the light (4d: Ru, Rh and Pd) and heavy (5d: Os, Ir and Pt) metals of the platinum group are intert towards carbon (nitrogen) and do not form double nitride (carbide) phases. Starting with the year 2004, a series of novel crystalline nitrides and carbides of platinum group metals was synthesized using modern high-pressure and high-temperature methods, film technologies *etc*.[43–46] A distinctive feature of the new phases (*e.g*., dinitrides PtN_2, IrN_2, OsN_2 and PdN_2) is a record-high (for d-metal nitrides) content of nitrogen. In addition, the mechanical properties [*e.g*., high compression moduli (B) and low compressibilities] of some dinitrides of platinum group metals appear to be quite interesting and promising for technological applications. For instance, the experimentally determined B modulus of IrN_2 [$B \approx 428$ GPa (Ref. 46)]

D V Suetin, I R Shein, A L Ivanovskii Institute of Solid State Chemistry, Ural Branch of the Russian Academy of Sciences, ul. Pervomaiskaya 91, 620990 Ekaterinburg, Russian Federation. Fax 7 (343) 374 44 95, tel. (7-343) 362 31 15, e-mail: suetin@ihim.uran.ru (D V Suetin), shein@ihim.uran.ru (I R Shein), tel. 7 (343) 374 53 31, e-mail: ivanovskii@ihim.uran.ru (A L Ivanovskii)

Received 19 February 2010
Uspekhi Khimii **79** (7) 672 – 696 (2010); translated by A M Raevskiy

is only 3% lower than that of diamond [$B \approx 440$ GPa (Refs 47 and 48)].

High potential of the systems comprised of heavy 4d- and 5d-metals (many of them have high compression moduli B) and light sp-nonmetals (B, C, N and O, which can form strong covalent bonds) for the search for materials with improved mechanical properties (high hardness, low compressibility) can be explained using the following simple model. The compression and shear (G) moduli are related to the density of valence electrons (N)[49]

$$\rho_e = \frac{N}{V_m},$$

where V_m is the molar volume, in such a manner:

$$B \approx \rho_e^l,$$

$$G \approx \rho_e^k,$$

where $l \approx 1.25$ and $k \approx 1.47$. The 'design principles' of superhard materials are as follows: the desired material should be similar to an isotropic material, have the highest possible density of valence electrons, covalent atom–atom bonds and be characterized by a minimum dislocation mobility.[50] Thus, one can expect manifestation of improved mechanical properties in covalent compounds of heavy d-metals (in particular, platinum group metals with high electron density) with light sp-elements.

In this context, tungsten carbides and nitrides are considered[51,52] as 'boundary phases' between the family of novel carbides (nitrides) of platinum group metals (see above) and 'classical' carbides and nitrides of Group IV and V d-metals.

The aforesaid predetermined the setting of studies on the peculiar features of the electronic structure, nature of chemical bonding and simulation of the properties of tungsten carbides and nitrides and more complex systems based on them using computational methods of quantum chemistry and computer-assisted materials science. Note that in the early stage of these investigations the emphasis was placed on the investigations of the electronic properties of two polymorphs of tungsten monocarbide, namely, hexagonal and cubic WC (h-WC and c-WC, respectively). The results obtained in these studies were summarized in Refs 10 and 33.

Recently, intensive research in the field of synthesis, materials science and simulation of novel tungsten-containing carbide and nitride phases has been continued.

For instance, the hardness and abrasion resistance of W_2C–(Co,Ni) alloys,[53] the effect of W_2C additives on the operating properties of WC/M composites and coatings,[54–57] the catalytic behaviour of W_2C,[58–60] and atom-vacancy ordering in tungsten subcarbide[61] were studied. Attempts to prepare and study the properties of W_2C nanopowders were made.[62–64] Studies[65–70] on the ternary system W–Al–C led to the synthesis of solid solutions (aluminocarbides $W_{1-x}Al_xC_y$) whose formation obeys an unusual (for this group of compounds) type of substitution, where atoms of the p-element (Al) occupy sites in the d-metal (W) sublattice. The introduction of aluminium into WC causes a significant decrease in the density of the starting WC, but its strength properties remain unchanged.[65] The aluminocarbide solid solutions thus obtained retain the hexagonal structure of the binary carbide WC.

In addition to these and many other experimental data on the novel materials based on tungsten carbides and nitrides, there is a great body of information on their electronic structure and properties which was obtained using computer simulation methods.

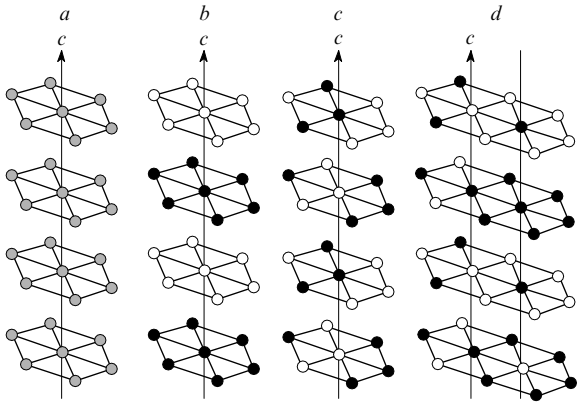
In this review we summarize the results obtained since the year 2000 in theoretical studies on the electronic structure, the nature of chemical bonding and some physicochemical properties of tungsten carbides (W_2C, WC) and nitrides (W_2N, WN, WN_2, WN_3) as well as ternary compounds and solid solutions including carbonitrides ($WC_{1-x}N_x$), aluminocarbides ($W_xAl_yC_z$), ternary carbides and nitrides with the perovskite structure (M_3WC, W_3MC and W_3MN, where M is a d-metal), η-phases (M_3W_3C and M_6W_6C) and some hypothetical compounds designed by modern *ab initio* computational methods. Attention has been paid to the potential of these methods in the analysis and prediction of structural states, phase stability and the elastic and magnetic properties of tungsten-containing systems.

II. Tungsten carbides

Two main phases known to date tn the W–C system include tungsten subcarbide (W_2C) and tungsten monocarbide (WC), each having a number of polymorphs. The phase diagram of the W–C system and the state-of-the-art in experimental studies on the physicochemical properties of tungsten carbides have been reviewed.[33]

1. Tungsten subcarbides

At present, four W_2C polymorphs (so-called α-, β-, γ- and ε-subcarbides[33]) differing in the type of distribution of carbon atoms over octahedral interstices of the metal sublattice (Fig. 1) are known. For instance, in the structure of γ-W_2C, carbon atoms randomly (with 50% probability) fill sites in the carbon sublattice. The structure of rombohedral α-W_2C comprises layers of carbon atoms and vacancies alternating along the c axis. In the β-W_2C and ε-W_2C



● *1*, ○ *2*, ● *3*.

Figure 1. Distribution types of carbon atoms and carbon vacancies in the structures of W_2C polymorphs.[33]
γ (*a*), α (*b*), β (*c*), ε (*d*); C atom (*1*), vacancy (*2*) and positions (*3*) of carbon sublattice γ-W_2C randomly filled with carbon atoms (with a 50% probability).

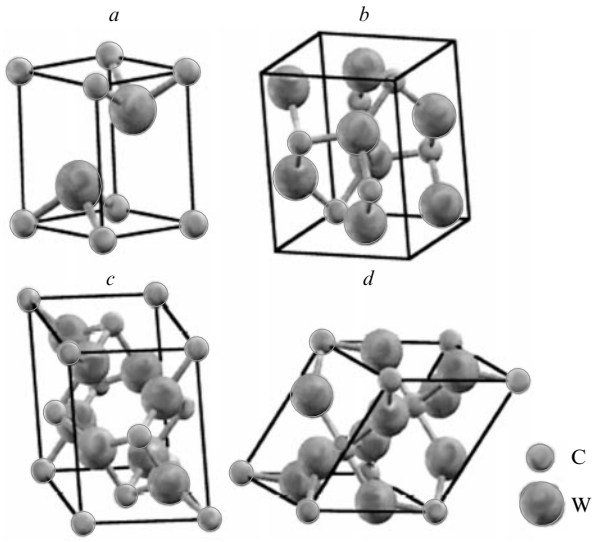


Figure 2. Fragments of the crystal structures of the polymorphs of the lower tungsten carbide W_2C.[71]
α (*a*), β (*b*), γ (*c*), ε (*d*).

polymorphs, carbon atoms and vacancies are distributed over all planes of the nonmetal sublattice in some ordered manner.

Recently, the structural, electronic and some other properties of the α-, β-, γ- and ε-subcarbides of the chemical formula W_2C were for the first time analyzed in the framework of *ab initio* methods of energy band theory.[71, 72] Fragments of the crystal lattices of the calculated W_2C polymorphs are shown in Fig. 2. The theoretical [71, 72] structural parameters (Table 1) agree with the experimental data. Analysis of the calculated densities of all W_2C polymorphs (see Table 1) showed that $\rho_{theor}(W_2C)$ is 8% – 9% higher than that of the monocarbides WC and decreases in the following order:

$$\beta\text{-}W_2C > \gamma\text{-}W_2C > \varepsilon\text{-}W_2C > \alpha\text{-}W_2C.$$

A characteristic feature of the electronic spectra of all W_2C polymorphs is the presence of groups of low-energy bands composed mainly of C2s states in the energy interval from −15 to −12 eV below the Fermi level ($E_F = 0$ eV) and groups of filled energy bands with the major contributions from the C2p and W5d states near the Fermi level (Fig. 3). The Fermi level is in the region of the W5d-like

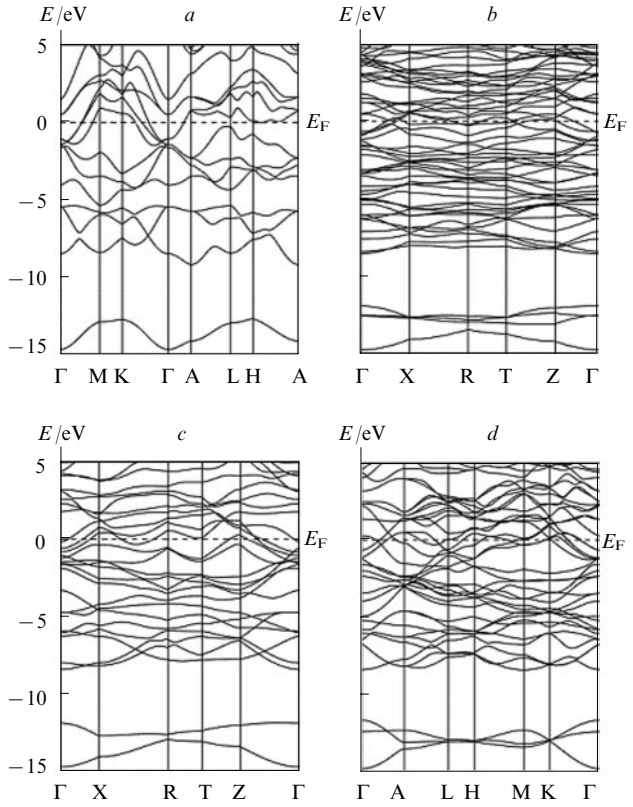


Figure 3. Energy band structures of the polymorphs of lower tungsten carbide W_2C.[72]
α (*a*), β (*b*), γ (*c*), ε (*d*).

bands, which predetermines the metal-like properties of all W_2C polymorphs. The total and partial densities of states (DoS) at the Fermi level $N(E_F)$ are listed in Table 2. As can be seen, for all W_2C polymorphs the maximum contributions to $N(E_F)$ come from the W5d states. The distribution type of carbon atoms in the α-, β-, γ- and ε-subcarbide structures significantly affects the $N(E_F)$ values which can differ by up to 30%; the maximum $N(E_F)$ value was determined for ε-W_2C. Table 2 also lists the theoretical estimates of the low-temperature heat capacity coefficients (γ) and the Pauli paramagnetic susceptibility (χ); both parameters decrease in the order [72]

$$\varepsilon\text{-}W_2C > \gamma\text{-}W_2C > \beta\text{-}W_2C > \alpha\text{-}W_2C.$$

Table 1. Structural types, space groups, optimized lattice constants (*a*, *b* and *c* /nm) and theoretical densities (ρ_{theor} /g cm^{-3}) of polymorphs of lower tungsten carbide W_2C.[71, 72]

Polymorph of W_2C	Structural type	Space group	*a*	*b*	*c*	ρ_{theor}
α	*anti*-CdI_2	*P*-3*m*1	0.3057	–	0.4697	16.585
			(0.3001)		(0.4728)	
β	PbO_2 or	*Pbcn*	0.4759	0.6097	0.5227	16.628
	Mo_2C (ζ-Fe_2N)		(0.4728)	(0.6009)	(0.5193)	
γ	W_2C	$P6_3/mmc$	0.3033	0.5281	0.4741	16.612
			(0.3002)		(0.475)	(17.34)
ε	ε-Fe_2N	*P*-31*m*	0.5253	–	0.4772	16.586
			(0.5190)		(0.4724)	

Note. Experimental values of the lattice constants [33] and ρ_{theor} (Ref. 7) are given in parentheses.

Table 2. The total and partial densities of states at the Fermi level [$N(E_F)$, $N^l(E_F)$], low-temperature heat capacity coefficients (γ/mJ K^{-2} mol^{-1}) and the Pauli paramagnetic susceptibility ($\chi/10^{-4}$ emu mol^{-1}) for polymorphs of lower tungsten carbide W_2C.[71,72]

Polymorph of W_2C	Density of states at the Fermi level, state per eV per atom			γ	χ
	N^{C2p}	N^{W5d}	$N(E_F)$		
α	0.030	0.378	0.693	3.26	0.45
β	0.038	0.386	0.736	3.47	0.48
γ	0.041	0.423	0.826	3.89	0.53
ε	0.018(1) } see [a]	0.463	0.892	4.21	0.58
	0.019(2) }				
	0.019(3) }				

[a] For three types of nonequivalent carbon atoms in the structure of ε-W_2C.

Analysis of the densities of electronic states of the subcarbide polymorphs showed[71] that the common p–d hybrid band (in the region from −9 eV to E_F) can be divided into two regions, *viz*., the lower region (from −9 to −4.5 eV) with predominant contributions of the C2p states participating in the formation of p–d covalent bonds W−C and the upper region (from −4.5 eV to E_F) with the contributions from the W5d states responsible for the W−W bonds in the metal sublattice of W_2C.

When describing phase equilibria in the W−C system and the properties of phases formed in this system, it is of crucial importance to determine the relative stabilities of tungsten carbide polymorphs and, in particular, to explore interrelations between possible distribution types of carbon atoms in the nonmetal sublattice of tungsten subcarbide and the relative stabilities of its polymorphs. Such estimates were made[72] using the calculated energies of formation (E_{form}) of phases in the formal reactions

$$2\,W + C^g \longrightarrow W_2C.$$

The energies of formation were determined from the relation

$$E_{form}(W_2C) = E_{tot}(W_2C) - [2\,E_{tot}(W) + E_{tot}(C^g)],$$

where $E_{tot}(W_2C)$, $E_{tot}(W)$ and $E_{tot}(C^g)$ are the total energies of tungsten subcarbides, metallic tungsten and graphite, respectively, obtained from *ab initio* calculations. In this approach, negative E_{form} values indicate that the formation of tungsten carbides is energetically favourable compared to a mechanical mixture of the starting reactants ($W + C^g$). *Vice versa*, at $E_{form} > 0$ the corresponding carbides should be treated as unstable systems. The results obtained suggest that the stable phases include ε-W_2C ($E_{form} = -0.044$ eV per formula unit) and β-W_2C ($E_{form} = -0.017$ eV per formula unit), whereas γ-W_2C and α-W_2C are characterized by positive values of E_{form} and should therefore be considered metastable.

An experimental study[33] showed that the ordered and disordered W_2C polymorphs often coexist with one another and with metallic tungsten and a higher carbide WC. In addition, W_2C is characterized by a rather wide homogeneity region from 25 at.% to 33 at.% of carbon.[33] Thus, the results obtained in the simulations[71,72] of 'perfect' tungsten subcarbides represent only a first step towards the description of the microscopic properties of such systems.

2. Tungsten monocarbides

There are two polymorphs of tungsten monocarbide WC,[1–7] a low-temperature hexagonal (h-WC; it forms a specific structural type) and a metastable, high-temperature cubic one (B1-type c-WC) (Fig. 4). In the stable phase h-WC (space group *P*-6*m*2), the carbon and tungsten atoms form simple hexagonal sublattices, which alternate as follows: ... *ABAB*... . Carbon atoms occupy the centres of trigonal prismatic interstices in the metal sublattice. Tungsten atoms occupy the positions 1*a* with the coordinates (0; 0; 0) while carbon atoms occupy the positions 1*d* with the coordinates (1/3; 2/3; 1/2). The high-temperature phase of c-WC has a simple cubic structure (space group *Fm*-3*m*) in which carbon atoms occupy octahedral interstices in the fcc sublattice of tungsten. The atomic positions in the lattice are as folows: W (0; 0; 0) and C (1/2; 1/2; 1/2).

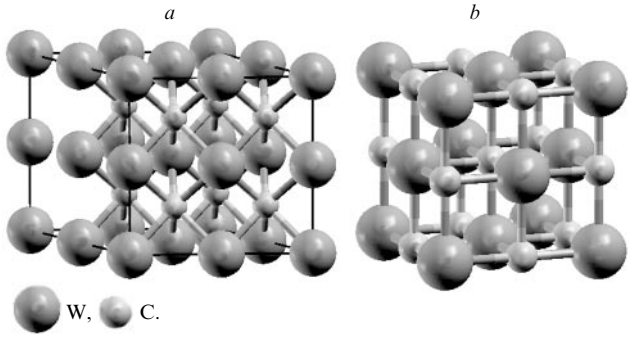


Figure 4. Fragments of the crystal structures of hexagonal (*a*) and cubic (*b*) polymorphs of tungsten monocarbide.

Both WC polymorphs have been studied in detail by *ab initio* methods.[72–86] Initially,[73–83] investigations were focussed on the peculiar features of the electronic spectra of h-WC and c-WC. It was established that the electronic spectra of both polymorphs are by and large similar (Fig. 5). The filled energy bands form two main groups separated by the forbidden gap. The lowest (quasi-core) energy band is mainly composed of C2s states, the next energy band has a mixed character, being composed of C2p and W5d states. The Fermi level crosses the W5d bands. On going from h-WC to c-WC the C2p–W5d valence band is

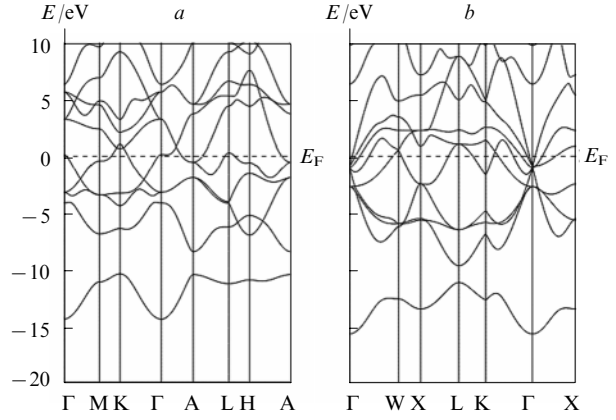


Figure 5. Energy band structures of hexagonal (*a*) and cubic (*b*) polymorphs of tungsten monocarbide.[85]

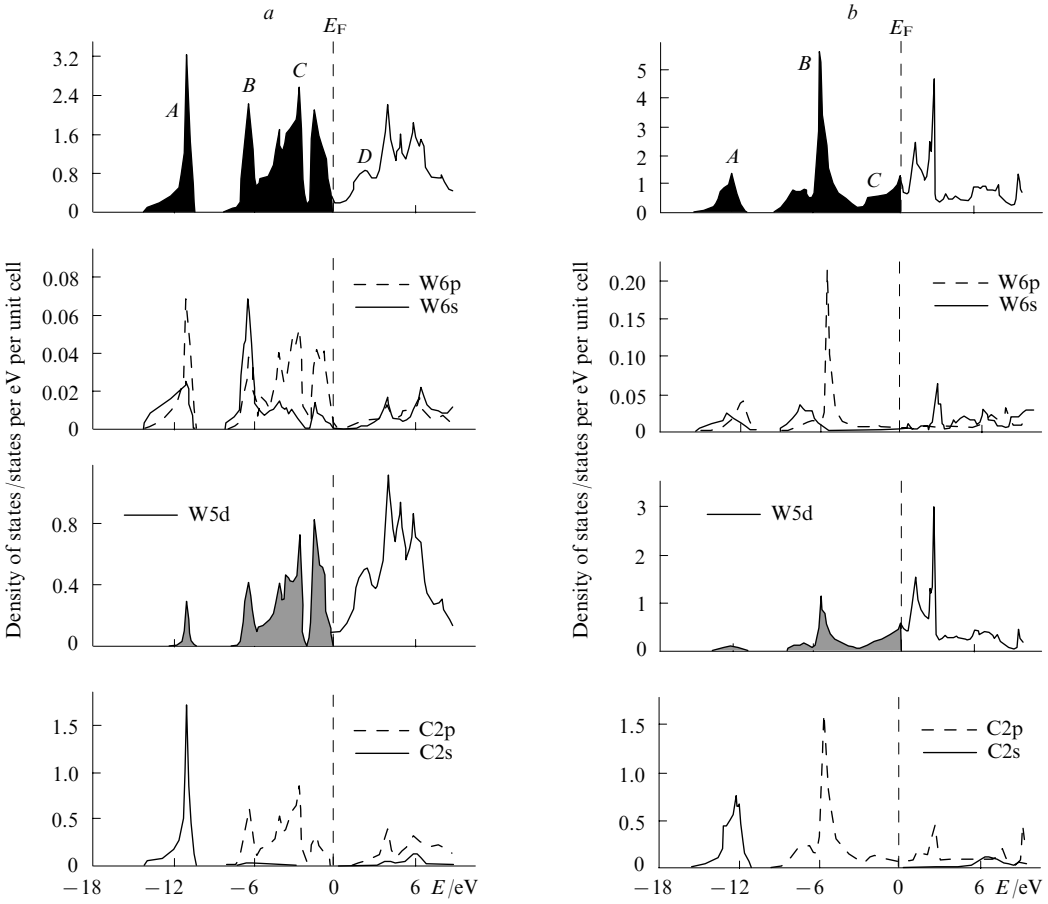


Figure 6. The total and partial densities of states in hexagonal (*a*) and cubic (*b*) polymorphs of WC.[85]

broadened and the total width of the C2s – E_F valence band increases.

The structure of the electronic spectra of WC polymorphs becomes clearer when analyzing the distributions of the total and partial densities of states (Fig. 6). As can be seen, for h-WC the low-lying energy band *A* corresponds to the C2s band and is in the energy interval from −14.5 to −10.3 eV below E_F. The next group of energy bands (*B* band) is composed of mixed C2p and W5d states. The filled energy band *C* near the Fermi level (from −2.5 eV to E_F eV) is mainly composed of W5d states. The Fermi level of h-WC crosses the W5d-like bands and is near the DoS minimum between the bonding (*C*) and antibonding (*D*) states, which suggests that this polymorph is stable.

In the cubic tungsten monocarbide, the low-lying energy band *A* is also composed of C2s states and separated from the next energy band *B* (here, the major contributions come from the C2p and W5d states) by a forbidden gap of 1.7 eV (see Fig. 6).

Interatomic interactions in h-WC and c-WC are of mixed type including ionic, covalent and metallic components. The W–W metal–metal bond is formed involving delocalized W5d states with energies near the Fermi level. The ionic component is due to partial transfer of the charge density between tungsten and carbon atoms because the electronegativities of the elements are different ($EN^W = 2.36$ and $EN^C = 2.55$). Finally, the covalent bond W–C is due to the overlap of the C2p and W5d states. The charge density maps (Fig. 7) suggest directed covalent

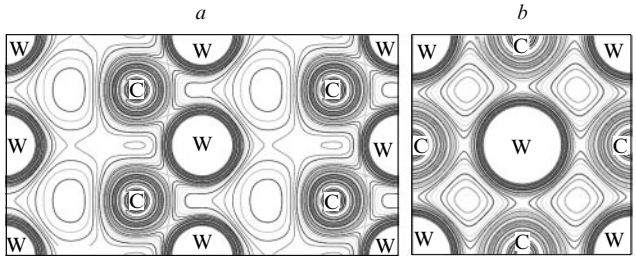


Figure 7. The charge density distribution for the valence states of hexagonal WC in the (110) plane (*a*) and of cubic WC in the (100) plane (*b*).[85]
Contours are drawn with an increment of 0.05 e Å^{-3}.

bonds W–C in these phases. As can be seen, h-WC (not c-WC!) is characterized by a higher concentration of the electron density along the W–C bonds, which indicates strengthening of the covalent bonds in the hexagonal phase.

The conclusions about the relative stabilities of the h-WC and c-WC phases, which follow from the analysis of the energy band structure, were confirmed by the results of calculations of their cohesive energies (E_{coh})[85,87] determined as the differences between the total energy of carbide (E_{tot}) and the sum of the total energies of isolated atoms (E_{at}):

$$E_{coh} = E_{tot}(WC) - [E_{at}(W) + E_{at}(C)].$$

The calculated cohesive energies are E_{coh}(h-WC) = −21.38 eV and E_{coh}(c-WC) = −20.48 eV per formula unit. Yet another method for evaluating the relative stabilities of WC polymorphs is based on calculations of the energies of their formation (E_{form}). These energies were estimated [72, 83] using the formal reaction

$$W + C^{g} \longrightarrow \text{h-WC, c-WC}$$

as

$$E_{form}(\text{h-WC, c-WC}) = E_{tot}(\text{h-WC, c-WC}) - [E_{tot}(W) + E_{tot}(C^{g})],$$

where E_{tot}(h-WC, c-WC), E_{tot}(W) and $E_{tot}(C^{g})$ are respectively the total band energies of tungsten monocarbides, metallic tungsten and graphite. The results obtained [85] are as follows: E_{form}(h-WC) = −0.34 and E_{form}(c-WC) = +0.56 eV per formula unit, which again suggests stability of the hexagonal phase and a metastable character of the cubic WC.

In addition to the electronic properties, the mechanical properties of WC were studied,[72–102] which to a great extent determine the fields of application of this carbide and materials based on it. Modern *ab initio* theoretical studies involve numerical calculations of the elastic constants (C_{ij}) of crystals, which are determined by expanding the total energy of the crystal $E(V,\alpha)$ into a Taylor series over a small deformation parameter α.[88, 89] The five independent constants for h-WC and three for c-WC are listed in Table 3.

Table 3. Elastic constants (GPa) for hexagonal and cubic polymorphs of WC.

C_{11}	C_{12}	C_{13}	C_{33}	C_{44}	Ref.
h-WC phase					
772.8	209.9	157.8	960.6	302.2	85
711.8 [a]	250.7 [a]	263.6 [a]	959.5 [a]	323.8 [a]	92
720.0	254.0	267.0	972.0	328.0	93
c-WC phase					
706.5	191.4	–	–	151.6	83

[a] Experimental data.

The C_{ij} values can be used to evaluate the mechanical stability of crystals. The stability conditions [88] are as follows:

for hexagonal crystals,

$$C_{11} > 0, (C_{11} - C_{12}) > 0, C_{44} > 0, (C_{11} + C_{12})C_{33} - 2(C_{12})^2 > 0;$$

and for cubic crystals,

$$(C_{11} - C_{12}) > 0, (C_{11} + 2C_{12}) > 0, C_{44} > 0.$$

From the data in Table 3 it follows that these conditions hold for h-WC and c-WC.

The elastic behaviour of materials is often described using the uniform compression, shear and Young (Y) moduli and the Poisson ratio (ν). For single crystals, these parameters can be determined using the constants C_{ij} in the framework of, *e.g.*, Voigt (V) (Ref. 94) or Reuss (R) approximations.[95]

The B and G moduli of h-WC and c-WC are listed in Table 4. The uniform compression and shear moduli of c-WC are lower than those of h-WC. For the compressibilities of these phases one has

$$\beta(\text{h-WC}) < \beta(\text{c-WC}).$$

Table 4. The uniform compression moduli and shear moduli of the hexagonal and cubic polymorphs of WC: results of calculations [78, 79, 85, 98, 99] and experimental data.[92, 100–102]

B/GPa	G/GPa	Ref.	B/GPa	G/GPa	Ref.
h-WC phase					
384.2	297.5	85	383	304	100
391		98	480		101
375		99	413		78
431		92	329		102
c-WC phase					
363.1	194.0	85	390		79
375		75			

In turn, for each polymorph one has $B > G$, *i.e.*, the mechanical stability of a polymorph is limited by the shear modulus.

A key parameter for characterization of the mechanical behaviour of materials is the brittleness. Often, the B/G ratio is used as a semiempirical criterion for the brittle–plastic transition.[97] According to this model, a substance is brittle if $B/G < 1.75$. For h-WC, one has $B/G \approx 1.3$,[85] *i.e.*, this is a brittle material. For c-WC, one has $B/G \approx 1.9$ (Ref. 85); the plasticity of c-WC is higher than that of h-WC.

The elastic parameters of varous ceramics (polycrystalline systems comprising aggregated mixtures of randomly oriented microcrystallites) are evaluated by averaging the values obtained according to Voigt and Reuss. This is achieved using the Voigt–Reuss–Hill (VRH) approximation [96] leading to the averaged compression modulus

$$B_{VRH} = \frac{1}{2}(B_V + B_R)$$

and shear modulus

$$G_{VRH} = \frac{1}{2}(G_V + G_R).$$

Knowing B_{VRH} and G_{VRH}, the Young modulus and the Poisson ratio for polycrystals can be determined with ease:

Table 5. Theoretical values of some elastic parameters of polycrystalline ceramics h-WC and c-WC calculated in the Voigt–Reuss–Hill approximation: compression moduli (B_{VRH}/GPa), shear moduli (G_{VRH}/GPa), compressibilities (β/GPa^{-1}), Young moduli (Y_{VRH}/GPa) and Poisson ratios (ν).

B_{VRH}	G_{VRH}	β	Y_{VRH}	ν	Ref.
h-WC polymorph					
382.4	294.6	0.002615	703.2	0.194	85
(427)		(0.002342)			92
			703		103
			(668.4–713.8)	(0.24)	104
				0.185	101
c-WC polymorph					
363.1	187.7	0.002754	480.4	0.279	85

Note. Experimental data are given in parentheses.

$$Y_{\mathrm{VRH}} = \frac{9B_{\mathrm{VRH}}G_{\mathrm{VRH}}}{3B_{\mathrm{VRH}} + G_{\mathrm{VRH}}},$$

$$v = \frac{3B_{\mathrm{VRH}} - 2G_{\mathrm{VRH}}}{2(3B_{\mathrm{VRH}} + G_{\mathrm{VRH}})},$$

The results of calculations of these parameters are listed in Table 5. It is known that the Poisson coefficients of covalently bound materials are rather small ($v \approx 0.1$).[105] For the WC polymorphs, the v values lie in the interval from 0.194 (h-WC) to 0.296 (c-WC),[85] *i.e.*, the hexagonal monocarbide WC should be characterized by the largest contribution of the covalent bond to the interatomic interaction.

III. Tungsten nitrides

In the W–N system, there are three main phases, namely, tungsten subnitride (W_2N), tungsten mononitride (WN) and tungsten dinitride (WN_2). Tungsten mononitride belongs to the best studied phases; there are a low-temperature hexagonal phase with the WC-type structure (h-WN) and a high-temperature cubic B1-type phase (c-WN).[1,3,7] Lower tungsten nitrides $WN_{x<1}$ are studied much poorer. In particular, the formation of the W_2N phase at $0 < N:W < 1$ was established. This subnitride has a simple cubic (B1-type) lattice, where tungsten atoms occupy the positions 4*a* (0; 0; 0) while nitrogen atoms randomly fill 50% of the 4*b* positons (1/2; 1/2; 1/2). The properties of W_2N were studied.[106–118] Experimental data on higher tungsten nitrides ($WN_{x>1}$) are limited to the early studies[119,120] on the synthesis and structural characterization of dinitride W_3N_6.

1. Tungsten subnitride

Recently, the first study of peculiar features of the electronic properties of W_2N using a 12-atom W_8N_4 unit cell in the B1-type structure with 50% vacant sites in the N-sublattice was reported.[121] The value of the lattice constant $a(W_2N) = 0.4199$ nm is in reasonable agreement with the experimental data (0.4128 nm)[5] and smaller than that of the B1-type cubic mononitride: a(c-WN) = 0.4362 nm. Therefore, the appearance of vacancies in the N-sublattice of the cubic phase of WN is accompanied by compression of the crystal lattice. Note that a similar effect is also characteristic of some other cubic transition metal carbides and nitrides in the corresponding homogeneity regions.[1–9] In addition, calculations[121] predict a high density of W_2N:

$$\rho_{\mathrm{theor}}(W_2N) > \rho_{\mathrm{theor}}(\text{h-WN}) > \rho_{\mathrm{theor}}(\text{c-WN}).$$

The key features of the energy band structure of W_2N (compared to mononitride WN) are due to narrowing of the N2s- and N2p-like energy bands (Fig. 8, bands *A* and *B*) and to the appearance of an additional peak of the density of the W5d states in the spectrum of W_2N (band *C*′), which corresponds to the formation of additional bonds between tungsten atoms near vacancies in the nitrogen sublattice in the subnitride. The Fermi level in W_2N crosses the W5d band, *i.e.*, the subnitride has a metal-like type of conductivity. Evaluation[121] of the cohesive energy (E_{coh}, eV per atom) of W_2N from the equation

$$E_{\mathrm{coh}}(W_2N) = E_{\mathrm{tot}}(W_2N) - [2E_{\mathrm{at}}(W) + E_{\mathrm{at}}(N)],$$

gave the following values:

Nitride	W_2N	h-WN	c-WN
$-E_{\mathrm{coh}}$	−10.94	−10.38	−9.98

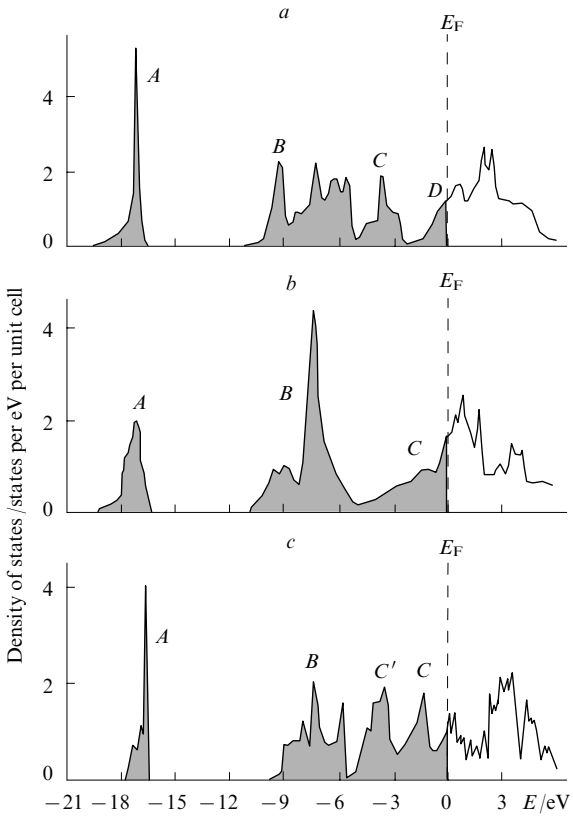


Figure 8. Total densities of states for hexagonal (*a*) and cubic (*b*) tungsten mononitride and for cubic W_2N (*c*).[121]

Qualitatively, the increase in the stability of cubic W_2N (compared to tungsten mononitrides) can be explained[121] by a decrease in $N_{\mathrm{tot}}(E_F)$, *i.e.*, by a decrease in the number of antibonding states and by the formation of new 'additional' W–W bonds.

2. Tungsten mononitrides

As mentioned above, tungsten mononitrides h-WN and c-WN are the best studied (including quantum chemical methods) phases in the W–N binary system.[84,85,122–126]

The lattice constants of h-WN and c-WN are listed in Table 6. The calculated densities of tungsten mononitrides are higher than those of tungsten monocarbides and lie in the range ~15.83–15.87 g cm^{-3} (Ref. 85), being close to the experimental value $\rho_{\mathrm{exp}} = 15.94$ g cm^{-3} (Ref. 122). The ρ_{theor} values increase in the following order of the WC and WN polymorphs:

c-WC < h-WC < c-WN < h-WN.

The total and partial densities of states of h-WN and c-WN (Fig. 9) give the idea of the corresponding energy spectra. For h-WN, the energy band *A* corresponds to the N2s band while the next energy band *B* is composed of hybridized N2p and W5d states. Then, the *C* and *D* bands with major contributions from W5d states are arranged in decreasing order of bond energy. In the cubic mononitride c-WN, the overall DoS distribution is similar to that found for h-WN; however, there is a single W5d band (*C*) near the Fermi level. On going from the hexagonal to cubic WN polymorph the density of states at the Fermi level increases from 1.191 to 1.478 state per eV per unit cell.[85]

Table 6. Lattice constants (a, b and c /nm), uniform compression moduli (B /GPa) and shear moduli (G /GPa) of tungsten mononitride polymorphs: results of calculations [84, 85, 123–126] and experimental data.[1]

Structural type	Lattice constants			B	G	Ref.
	a	b	c			
Mononitride h-WN						
WC	0.2865	—	0.2912	365.3	163.1	85
	0.2893	—	0.2826	—	—	1
	0.2829	—	0.2860	419	181.0	126
NiAs	0.2817	—	0.5693	416	281.0	126
TaN	0.5054	—	0.2873	—	—	126
CoSn	0.5078	—	0.2851	—	—	126
CrN	0.2804	0.4116	0.3381	—	—	126
Mononitride c-WN						
NaCl	0.4362	—	—	348.8	10.9	85
	0.436	—	—	394	—	123
	0.435	—	—	354		84
	0.4154	—	—	—	—	124
	0.420	—	—	—	—	125
ZnS	0.4596	—	—	—	—	126
CsCl	0.2674	—	—	—	—	126

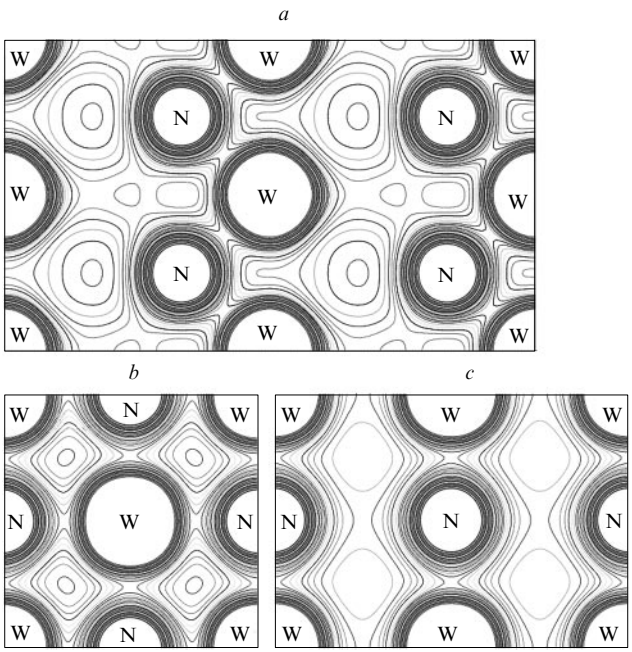


Figure 10. The charge density distribution for the valence states of hexagonal (a) and cubic (b, c) tungsten mononitride in the (110) (a, c), (100) (b) crystallographic planes.[85]
Contours are drawn with an increment of 0.05 e Å^{-3}.

Peculiarities of interatomic interactions in h-WN and c-WN are illustrated in Fig. 10. Both phases are characterized by the directed covalent bonds W—N involving the

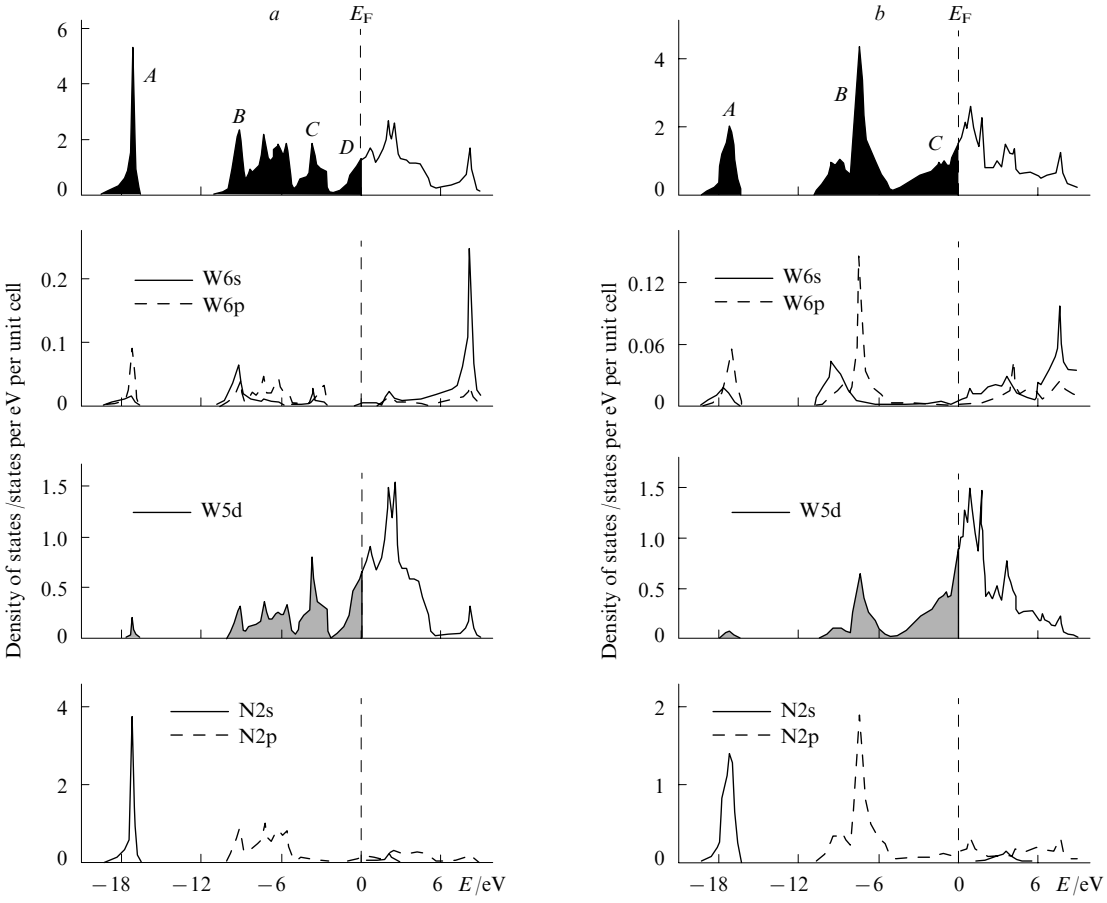


Figure 9. The total and partial densities of states for hexagonal (a) and cubic (b) WN.[85]

N2p and W5d hybridized states and the metal—metal bonds W—W. There are almost no N—N bonds. Compared to h-WN, the covalent (W—N) and metal—metal (W—W) bonds in c-WN are to some extent weakened.

The cohesive energy calculations for h-WN and c-WN using the expression

$$E_{coh} = E_{tot}(WN) - [E_{at}(W) + E_{at}(N)]$$

led to E_{coh}(h-WN) = −20.76 eV and E_{coh}(c-WN) = −19.96 eV per formula unit. Thus, the cubic phase is less stable than the hexagonal one (as in the case of tungsten monocarbides) and the stabilities of tungsten monocarbides and mononitrides change as follows:[85]

h-WC > h-WN > c-WC > c-WN.

Studies[85] of the mechanical behaviour of the h-WN and c-WN phases showed that the compression and shear moduli of h-WN are higher than those of c-WN (see Table 6).

Summing up, mention may be made of a comparative analysis[126] of some properties of eight WN polymorphs including h-WN and c-WN (see above) as well as hypothetical cubic (with the sphalerite and CsCl structural types), hexagonal (NiAs-, CoSn- and TaN-types) and orthorhombic (CrN-type) phases (see Table 6). The highest stability was predicted[126] for hexagonal WN (NiAs-type) characterized by the maximum calculated moduli B and G (see Table 6) and the lowest compressibility (Fig. 11). No experimental proof for these predictions is available at the moment.

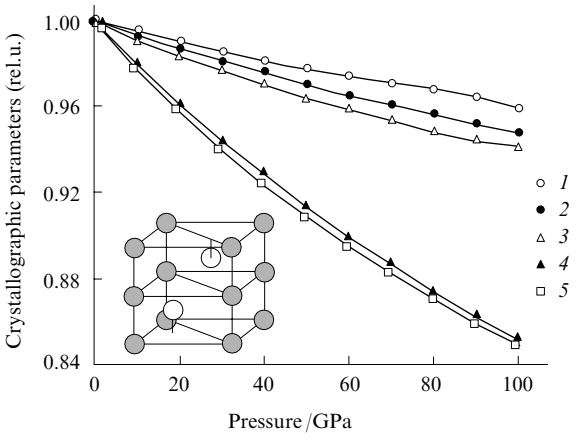


Figure 11. Pressure dependences of the crystallographic parameters of hypothetical hexagonal polymorph of WN (NiAs structural type) (inset: structural fragment) and diamond.[126]
Lattice constants c/c_0 (*1*), a/a_0 (*2*, *3*) and unit cell volumes V/V_0 (*4*, *5*) for WN (*1*, *3*, *5*) and diamond (*2*, *4*).

3. Tungsten di- and trinitrides

Recently, in connection with the discovery of interesting properties (*e.g.*, mechanical properties such as high elastic moduli and low compressibility) in the carbides and nitrides of platinum group metals (see a review[43]), tungsten di- and trinitrides (WN_2 and WN_3) have been a subject of theoretical studies[51, 52, 127, 128] including simulation of their electronic properties as well as structural and mechanical parameters. Six hypothetical WN_2 phases with the $P6_3/mmc$ and $P\text{-}6m2$ hexagonal structures,[52] as well as phases with a monoclinic IrP_2-type structure[128] and with the pyrite and fluorite,[127] baddeleyite (ZrO_2) and cottunite ($PbCl_2$)[51] structures were studied.

The equilibrium lattice constants and the electronic spectra were calculated; particular attention was paid to evaluation of the elastic constants C_{ij} and the compression and shear moduli. Analysis of the data listed in Table 7 shows that the maximum moduli B are predicted for the first two layered polymorphs with the hexagonal structure (Fig. 12). The Vickers microhardness test according to Ref. 129 gives for these polymorphs $H_V \sim 36.7$ GPa, which is higher than the corresponding values for such well-known hard materials as α-quartz (30.6 GPa) or β-Si_3N_4 (30.3 GPa). High hardness of these dinitrides is attributed[52] to the interactions between adjacent molecular layers ...(NWN)/(NWN)... due to strong covalent bonds N—N. According to calculations,[52] these phases are semiconductors [unlike the metal-like WN_2 polymorphs with the pyrite, fluorite,[127] and IrP_2 structures (Ref. 128)]; it is assumed that they can be synthesized at high pressures.

Hypothetical trinitride WN_3 (with TcP_3-type orthorhombic lattice) is a metal-like compound with chains of directed covalent bonds ...—W—N—N—N—... between

Table 7. The compression moduli and shear moduli of some hypothetical phases of tungsten dinitride.[52, 127, 128]

Space group	B /GPa	G /GPa
$P6_3/mmc$	364 (411)[a]	228 (252)
$P\text{-}6m2$	364 (412)	231 (255)
$Fm3m$	335	81
$P3m1$	325	112
$P21/c$	332	173

[a] In the generalized gradient approximation (GGA) of local electron density (LDA).[52]

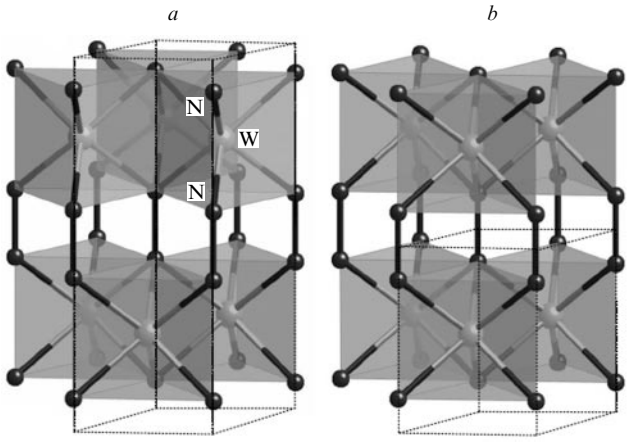


Figure 12. Fragments of hexagonal polymorphs of tungsten dinitride for which extremal strength properties were predicted.[52]
The neighbouring layers (NWN)/(NWN) interact through the formation of strong covalent bonds N—N. Space group: $P6_3/mmc$ (*a*) and $P\text{-}6m2$ (*b*).

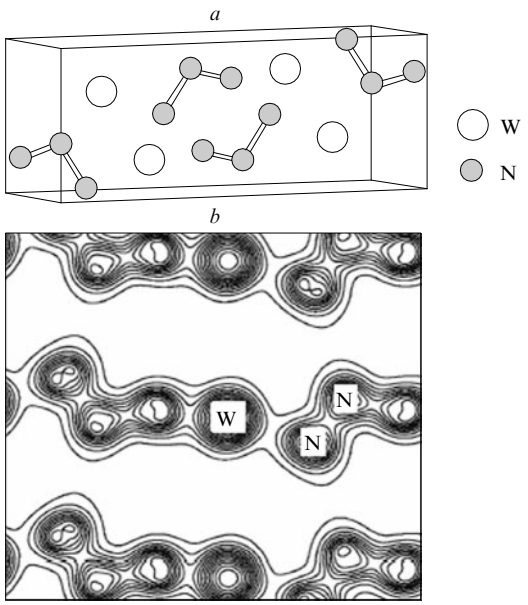


Figure 13. Fragment of the crystal structure of hypothetical WN_3 (TcP_3 structural type) (*a*) and the charge density map for WN_3 (*b*), which illustrates the formation of chains of directed covalent bonds ...–W–N–N–N–... .[128]

tungsten atoms and N_2 pseudodimers (Fig. 13).[128] The elastic moduli of WN_3 (B = 303 GPa and G = 156 GPa)[128] are lower than those of WN or WN_2 (see Tables 6 and 7).

IV. Ternary systems based on tungsten carbides and nitrides

In this Section we will consider the results of quantum chemical studies of the electronic structure, parameters of atom–atom interactions and some properties of ternary tungsten-containing systems, *viz*., solid solutions including carbonitrides ($WC_{1-x}N_x$), borocarbides ($WC_{1-x}B_x$) and boronitrides ($WN_{1-x}B_x$), aluminocarbides ($W_{1-x}Al_xC$), ternary phases including the so-called η-carbides (M_3W_3C and M_6W_6C, where M is a d-metal) and tungsten carbides and nitrides with the perovskite structure (M_3WC, W_3MC and W_3MN).

1. Tungsten carbonitrides

Unlike well-studied mutual solid solutions of cubic ($B1$-type) carbides and nitrides of 3d–5d-metals,[1–12] information on hexagonal tungsten carbonitrides ($WC_{1-x}N_x$) and oxycarbides ($WC_{1-x}O_x$) is scarce. In particular, tungsten carbonitrides with variable nitrogen content (from 1% to 20%) were synthesized,[130] as well as $WC_{1-x}N_x$ films were fabricated and some of their properties as coatings (diffusion barriers on metal ceramics) were studied.[131] More complex tungsten-containing carbonitride materials of the $(M_xW_y)C_{1-z}N_z$ type (M is a Group IV and V d-metal) proposed as cermets were also fabricated.[132, 133]

The electronic structures of hexagonal tungsten carbonitrides were studied[134] using 16-atom periodic supercells $W_8C_{8-m}N_m$ (m = 1, 2 and 4) for simulation of a series of tungsten carbonitrides with the formal stoichiometry $WC_{1-x}N_x$ (x = 0.125, 0.25 and 0.50). The dependence of the properties on possible mutual position of different-type atoms (N and C) in the nonmetal sublattice was studied taking a solid solution $WC_{0.75}N_{0.25}$ as an example. To this end, two nitrogen atoms in the model $W_8C_6N_2$ cell were located in three different ways, *viz*., (1) in close proximity within adjacent layers; (2) in close proximity within the same layer; and (3) at a long distance within adjacent layers. It was established that the $WC_{1-x}N_x$ ($x \leqslant 0.25$) solid solutions retain the hexagonal structure of the starting carbide upon introduction of low concentrations of nitrogen atoms into the WC lattice and that an increase in the N : C ratio leads to rhombohedral distortions. The phase transition from the hexagonal to rhombohedral phase depends on the N : C ratio and on the mutual position of these atoms in the lattice, *e.g*., the $WC_{0.75}N_{0.25}$ solid solution retains the hexagonal structure if nitrogen atoms (in the model cell) are in close proximity within adjacent layers. In other cases, the hexagonal lattice is transformed to rhombohedral one. As the N : C ratio increases, the lattice constants of the solid solution decrease [this is determined by the atomic radii R(C) = 0.077 nm > R(N) = 0.071 nm]; their dependences on the C : N ratio for $WC_{1-x}N_x$ deviated from those predicted by Vegard's rule (Fig. 14).

The dependences of the cohesive energies and parameters of the electronic spectrum [in particular, the density of states at the Fermi level, $N(E_F)$] of $WC_{1-x}N_x$ on the N : C ratio show a nonmonotonic behaviour (see Fig. 14).[134] In addition, the cohesive energy $WC_{1-x}N_x$ depends on the mutual ordering of carbon and nitrogen atoms in carbonitrides. It was assumed[134] that target control of the ordering

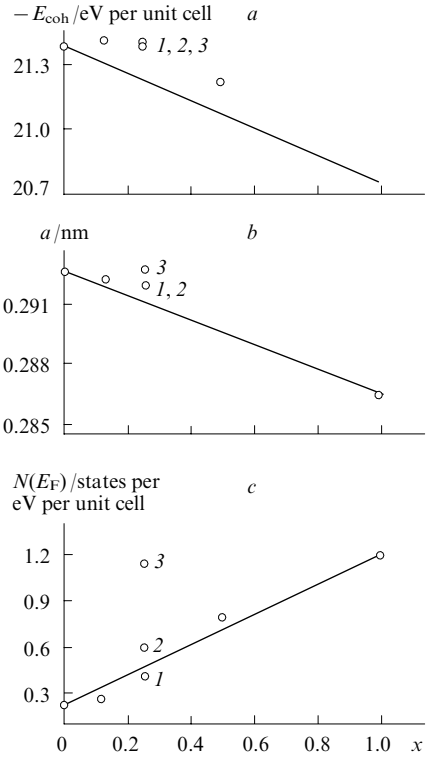


Figure 14. The concentration dependences of the lattice constant (*a*), cohesive energy (*b*) and total density of states at the Fermi level (*c*) for solid solutions $WC_{1-x}N_x$.[134]
For the carbonitride $WC_{0.75}N_{0.25}$ listed are the values corresponding to different mutual arrangement of nitrogen atoms (*1–3*, see text).

of the nonmetal atoms containing in tungsten carbonitrides may appear to be at least as efficient as variation of the chemical composition in modificaton of the properties of such systems.

2. Tungsten borocarbides and boronitrides

To reveal how the properties of hexagonal tungsten-containing solid solutions depend on the chemical composition and concentration of valence electrons, hypothetical tungsten borocarbide and boronitride ($WB_{0.5}C_{0.5}$ and $WB_{0.5}N_{0.5}$, respectively) were considered in addition to tungsten carbonitrides.[134] Whereas for tungsten carbonitrides $WC_{1-x}N_x$ the concentration of valence electrons increases with the N : C ratio

$$WC\ (10e) < WC_{0.875}N_{0.125}\ (10.125e) < < WC_{0.75}N_{0.25}\ (10.25e) < WC_{0.5}N_{0.5}\ (10.5e) < WN\ (11e),$$

tungsten borocarbide $WB_{0.5}C_{0.5}$ is characterized by an electron deficiency of 9.5 e while the concentration of valence electrons in $WB_{0.5}N_{0.5}$ (10 e) equals that of the parent carbide WC.

It was found[134] that the structures of $WB_{0.5}C_{0.5}$ and $WB_{0.5}N_{0.5}$ undergo rhombohedral distortions and the cohesive energies (in absolute values) of these solid solutions are much lower than those of tungsten carbonitrides. Analysis of the electronic structure showed[134] that boron-containing solid solutions lose their stability due to weakening of atom–atom bonds; the effect can clearly be monitored by comparing the electron density maps for $WC_{0.5}N_{0.5}$ and $WB_{0.5}C_{0.5}$ (Fig. 15).

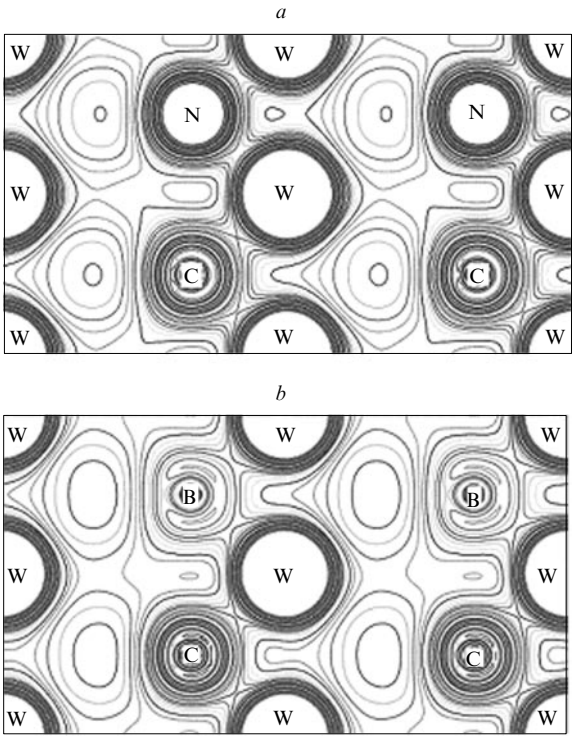


Figure 15. The charge density distribution for the valence states of $WC_{0.5}N_{0.5}$ (*a*) and $WB_{0.5}C_{0.5}$ (*b*) in the (110) plane.[134]
Contours are drawn with an increment of 0.05 e Å^{-3}.

3. Tungsten aluminocarbides

Sintering, hot pressing or mechanochemical treatment of W + Al + C mixtures or $W_{1-x}Al_x$ + C alloys led to the synthesis of novel solid solutions, *viz*., tungsten aluminocarbides of the general formula $W_xAl_yC_z$.[65–70] These methods allow one to prepare novel materials whose densities are much lower than that of the parent WC (*cf*. $\rho_{W_xAl_yC_z} = 8.99-9.44$ g cm^{-3}, $\rho_{WC} = 15.63$ g cm^{-3}), while the microhardness remains comparable with or is even higher than that of WC. Attempts to obtain $W_xAl_yC_z$ samples in the nano state (5-nm nanocrystallites[68]) and ceramic materials of more complex composition $W_xAl_yC_z$ + Co (Ref. 135) were reported.

Key features of the novel solid solutions $W_xAl_yC_z$ with the WC-type hexagonal structure include:

— occupation of sites in the d-metal (W) sublattice by the p-element (Al) atoms;

— considerable non-stoichiometry (to $z \approx 0.5$ for $W_xAl_yC_z$) with respect to the carbon sublattice, whereas the width of the homogeneity region of the parent WC is negligible.[33] In addition to the solid solutions mentioned above, it is assumed[136,137] that there exists an ordered phase in the W–Al–C system, namely, a hexagonal aluminocarbide W_2AlC (space group $P6_3/mmc$) belonging to a broad class of the so-called nanolaminates (also known as *H*-phases).[11,138–142] The lattice of W_2AlC is built of W_2C blocks in such a manner that each carbon atom is in octahedral coordination $\{CW_6\}$. In turn, adjacent W_2C blocks are separated by planar networks of aluminium atoms. Fragments of the crystal structures of the solid solutions $W_xAl_yC_z$ (exact chemical composition is $W_{0.5}Al_{0.5}C$) and nanolaminate W_2AlC are shown in Fig. 16.

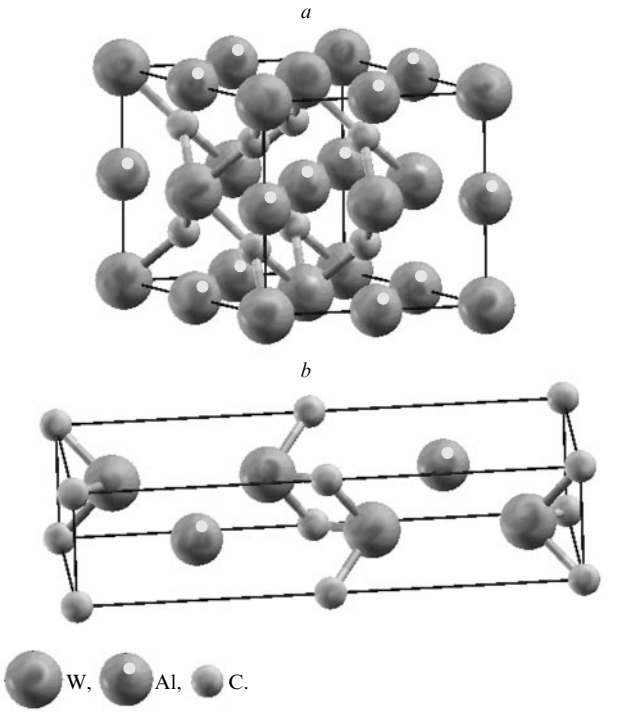


Figure 16. Fragments of the crystal structures of the solid solution $W_{0.5}Al_{0.5}C$ (*a*) and the layered phase W_2AlC (*b*).

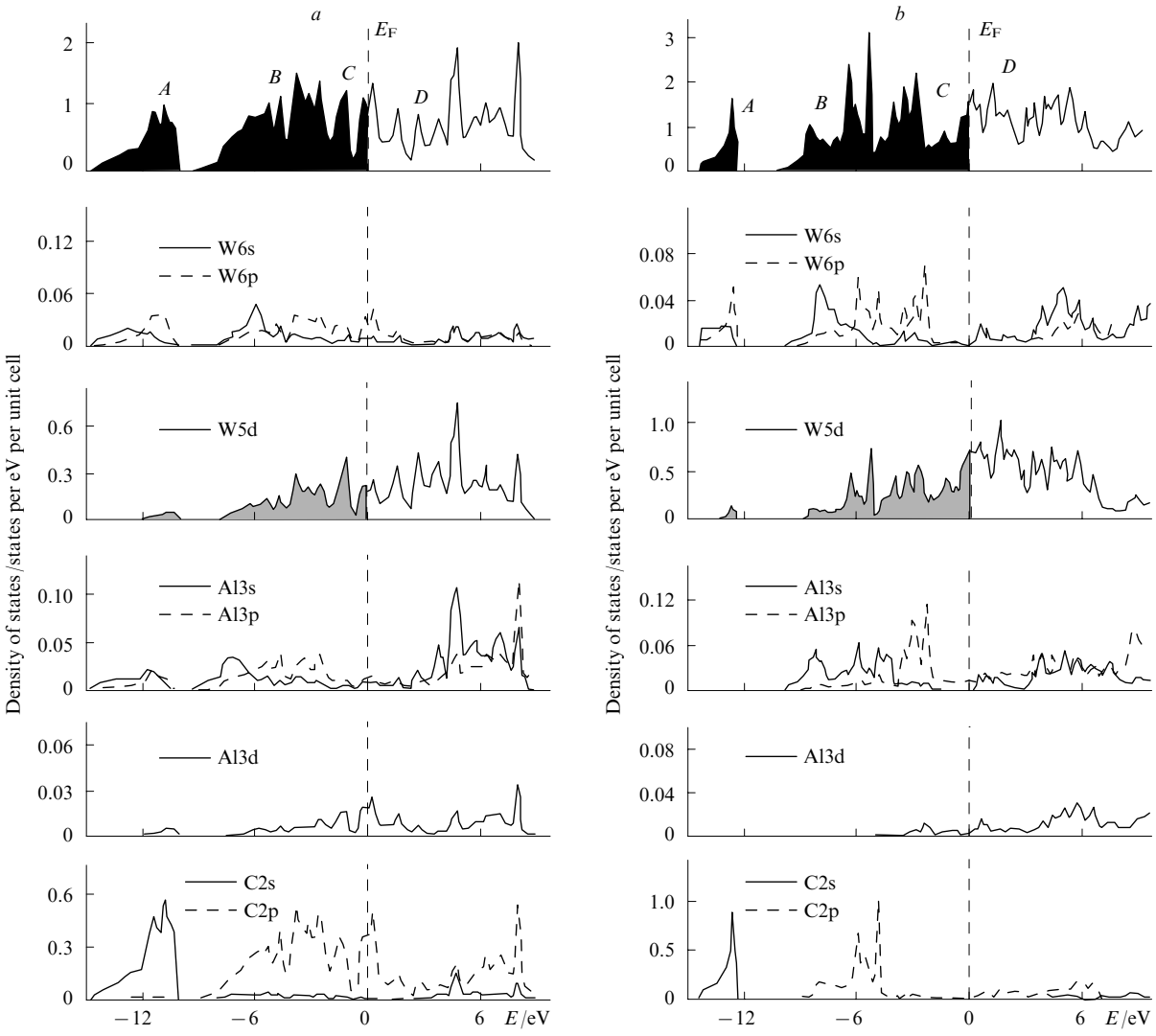


Figure 17. The total and partial densities of states of the solid solution $W_{0.5}Al_{0.5}C$ (*a*) and the layered phase W_2AlC (*b*).[143]

Specific features of the electronic structure of the $W_xAl_yC_z$ solid solutions (taking $W_{0.5}Al_{0.5}C$ as an example) were compared with those of double carbides WC and Al_4C_3 and an ordered ternary phase (aluminocarbide W_2AlC).[143] The distribution of the density of states (Fig. 17) shows that for $W_{0.5}Al_{0.5}C$ and W_2AlC the filled energy bands include four main bands from *A* to *D*. The bands *A* and *B* have the C2s and C2p character, respectively; they are separated by the band gap whose width is strongly dependent on the structure and chemical composition of each aluminocarbide ($W_xAl_yC_z$ or W_2AlC). The band *B* corresponds to hybridization of the C2p and W5d states, which suggests sufficiently strong covalent bonds W−C. The Al3s,p,d states make a much lower contribution to the total density of states in the energy interval from −9 eV to E_F compared to the W5d states; this predermines a relatively low degree of hybridization of the states Al3p and W5d, C2p. For $W_{0.5}Al_{0.5}C$, the bands *C* and *D* include the bonding and antibonding C2p states, whereas the W5d states dominate in these bands in the layered carbide W_2AlC. Unlike the semiconductor Al_4C_3, both aluminocarbides are expected to possess metal-like properties. Estimates of the Sommerfeld coefficients and the Pauli paramagnetic susceptibility suggest an increase in the 'metallic' character of carbides in the order

$$WC < W_{0.5}Al_{0.5}C < W_2AlC.$$

The stabilities of aluminocarbides $W_{0.5}Al_{0.5}C$ and W_2AlC were evaluated theoretically based on the results of calculations of the cohesive energies and energies of formation.[144] The cohesive energies of, *e.g.*, W_2AlC were calculated from the relationship

$$E_{oh}(W_2AlC) = E_{tot}(W_2AlC) - [2E_{at}(W) + E_{at}(Al) + E_{at}(C)],$$

where E_{tot} is the total energy of aluminocarbide and E_{at}(W,Al,C) are the total energies of corresponding atomic constituents in the free (neutral) state.

The E_{coh} values thus obtained determine the energy gain in the formation of a compound from free atoms and can be interpreted as the energy of chemical bonding. According to calculations,[144] $E_{coh} = -10.7$ eV for WC, −9.1 eV for W_2AlC and −7.8 eV per atom for $W_{0.5}Al_{0.5}C$, *i.e.*, the most stable phase is tungsten monocarbide with strong covalent bonds W−C in the $\{CW_6\}$ trigonal prisms. Among aluminocarbides, the most stable is the layered phase W_2AlC whose lattice also contains structural units

of WC, *viz*., $\{CW_6\}$ fragments. The least stable solid solution is $W_{0.5}Al_{0.5}C$ containing $\{CW_3Al_3\}$ fragments.

The energies of formation of aluminocarbides synthesized in different manner were estimated.[143, 144] For instance, W_2AlC can be synthesized (1) from simple components, *viz*., the metals [W and Al) and carbon (*e.g*., its most stable allotrope, graphite C^g] by the formal solid-phase reaction

$$2\,W + Al + C^g \longrightarrow W_2AlC;$$

(2) in the reactions involving a binary carbide

$$2\,WC + Al \longrightarrow W_2AlC + C^g$$

or

$$\frac{1}{3}\,Al_4C_3 + 2\,W \longrightarrow W_2AlC + \frac{1}{3}\,Al;$$

(3) in the reaction involving both binary carbides

$$2\,WC + Al_4C_3 \longrightarrow W_2AlC + 4\,C^g + 3\,Al; \quad \text{and}$$

(4) in the reaction involving the $W_{0.5}Al_{0.5}$ alloy and graphite

$$4\,W_{0.5}Al_{0.5} + C^g \longrightarrow W_2AlC + Al.$$

For these reactions, the corresponding energies of formation were calculated from the equations

$$E_{form}(W_2AlC) = E_{tot}(W_2AlC) - \\ -[2\,E_{tot}(W) + E_{tot}(Al) + E_{tot}(C^g)],$$

$$E_{form}(W_2AlC) = [E_{tot}(W_2AlC) + E_{tot}(C^g)] - \\ -[2\,E_{tot}(WC) + E_{tot}(Al)],$$

$$E_{form}(W_2AlC) = \left[E_{tot}(W_2AlC) + \frac{1}{3}E_{tot}(Al)\right] - \\ -\left[\frac{1}{3}E_{tot}(Al_4C_3) + 2\,E_{tot}(W)\right],$$

$$E_{form}(W_2AlC) = [E_{tot}(W_2AlC) + 3\,E_{tot}(Al) + 4\,E_{tot}(C^g)] - \\ -[E_{tot}(Al_4C_3) + 2\,E_{tot}(WC)],$$

$$E_{form}(W_2AlC) = [E_{tot}(W_2AlC) + E_{tot}(Al)] - \\ -[4\,E_{tot}(W_{0.5}Al_{0.5}) + E_{tot}(C^g)].$$

where E_{tot} are the total energies of the corresponding crystalline substances (tungsten, aluminium and graphite) and their compounds (binary carbides and aluminocarbide). Similar E_{form} calculations were also carried out for WC, Al_4C_3, $W_{0.5}Al_{0.5}$ and $W_{0.5}Al_{0.5}C$.

An analysis of the data of Table 8 suggests the following. Binary carbides WC and Al_4C_3, as well as $W_{0.5}Al_{0.5}$ are characterized by negative E_{form} values; therefore, these phases are stable. Contrary to this, both aluminocarbides in all reactions considered have $E_{form} \geqslant 0$; in other words, these phases are unstable and can be obtained under non-equilibrium conditions. Of course, a more correct simulation of the synthesis conditions of $W_{0.5}Al_{0.5}C$ and W_2AlC should take into account the effect of temperature and pressure. In addition, for each aluminocarbide the energy E_{form} depends strongly on the synthesis procedure. For instance, the synthesis of aluminocarbide $W_{0.5}Al_{0.5}C$ from elemental substances (tungsten, aluminum, graphite) is the most energetically favourable because in this case E_{form} has the minimum positive value. The synthesis of this phase from stable binary carbides WC and Al_4C_3 is the least energetically favourable. The energies E_{form} for the reactions involving a binary carbide (WC or Al_4C_3), and $W_{0.5}Al_{0.5}$ have intermediate values. These results are by and large in agreement with those of experiments[65–70] in which solid solutions $W_xAl_yC_z$ with the WC-type structure were synthesized by sintering of W, Al and graphite powders (or graphite and W–Al alloys) rather than binary carbides WC and Al_4C_3.

Table 8. Energies of formation of WC, Al_4C_3, $W_{0.5}Al_{0.5}$, $W_{0.5}Al_{0.5}C$ and W_2AlC in different model solid-phase reactions.[143]

Reaction	E_{form} /eV per atom
$\frac{1}{2}W + \frac{1}{2}Al + C^g \rightarrow W_{0.5}Al_{0.5}C$	+0.47
$WC + \frac{1}{2}Al \rightarrow W_{0.5}Al_{0.5}C + \frac{1}{2}W$	+0.64
$\frac{1}{3}Al_4C_3 + \frac{1}{2}W \rightarrow W_{0.5}Al_{0.5}C + \frac{5}{6}Al$	+0.55
$\frac{1}{2}WC + \frac{1}{2}Al_4C_3 \rightarrow W_{0.5}Al_{0.5}C + \frac{3}{4}Al + \frac{1}{2}C^g$	+0.67
$W_{0.5}Al_{0.5} + C^g \rightarrow W_{0.5}Al_{0.5}C$	+0.52
$2\,W + Al + C^g \rightarrow W_2AlC$	0.0
$2\,WC + Al \rightarrow W_2AlC + C^g$	+0.17
$\frac{1}{3}Al_4C_3 + 2\,W \rightarrow W_2AlC + \frac{1}{3}Al$	+0.04
$Al_4C_3 + 2\,WC \rightarrow W_2AlC + 4\,C^g + 3\,Al$	+0.29
$4\,W_{0.5}Al_{0.5} + C^g \rightarrow W_2AlC + Al$	+0.10
$W + C^g \rightarrow WC$	−0.17
$4\,Al + 3\,C^g \rightarrow Al_4C_3$	−0.07
$\frac{1}{2}W + \frac{1}{2}Al \rightarrow W_{0.5}Al_{0.5}$	−0.10

The results of E_{form} calculations for possible model reactions of the synthesis of nanolaminate W_2AlC (see Table 8) lead to similar conclusions. Here, for same-type reactions one has $E_{form}(W_2AlC) < E_{form}(W_{0.5}Al_{0.5}C)$, which characterizes the layered aluminocarbide W_2AlC as a highly stable compound compared to $W_{0.5}Al_{0.5}C$ (see above). In addition, the stability of solid solutions $W_{1-x}Al_xC$ increases as the parameter x decreases (W : Al ratio increases).

As mentioned above, $W_xAl_yC_z$ samples may have a large number of vacancies in the carbon sublattice ($z \geqslant 0.5$).[70] The results of simulation of non-stoichiometric tungsten aluminocarbide (solid solution $W_{0.5}Al_{0.5}C_{0.75}$) suggest[145] that a wide homogeneity region of these solid solutions is due to the stabilizing effect of C-vacancies because the introduction of such vacancies into $W_{1-x}Al_xC_y$ considerably reduces the density of states at the Fermi level. In addition, an analysis[145] of possible ordering types of carbon vacancies showed that 'clustering' of vacancies, which can initiate decomposition of solid solutions to individual phases, is energetically unfavourable and the preferred situation for vacancies is to be located at maximum distances from one another.

Nanolaminate W_2AlC and related phases M_2AlC (M = Ti, Zr, Hf, V, Nb, Ta, Cr and Mo) were studied to estimate the uniform compression moduli B[146, 147] and the compressibilities at pressures to 70 GPa.[136] Taking into account the character of the M_2C/Al interaction between adjacent layers, all M_2AlC phases can be divided into two groups, the so-called loosely bound phases (M = Ti, Zr, Hf) and the tightly bound ones where M are all other d-metals.[136, 146, 147] It was found that among these phases,

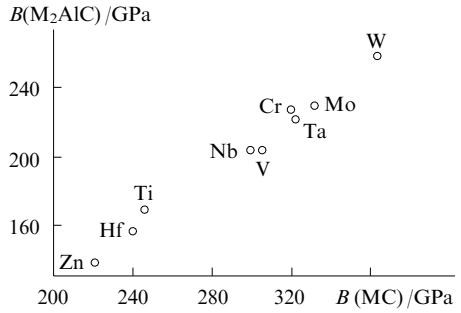


Figure 18. The uniform compression moduli of nanolaminates M_2AlC (M = Ti, Zr, Hf, V, Nb, Ta, Cr, Mo, W) plotted *vs.* *B* values of the corresponding metal monocarbides MC.[147]

W_2AlC is characterized by the maximum *B* value ($B > 250$ GPa) and the lowest compressibility (Fig. 18). This was explained[136] by the strongest M–C and M–Al bonds (and by minimum anisotropy of particular bonds) in W_2AlC compared to other M_2AlC phases.

Solid solutions $Nb_{2-x}W_xAlC$ ($0 < x < 2$) were studied.[137] According to calculations, doping of nanolaminate Nb_2AlC with tungsten causes a considerable (to 30%) increase in its elastic modulus. At the same time, one should take into account the fact that the introduction of tungsten into Nb_2AlC leads to a progressive decrease (in absolute value) in the energy of formation of this solid solution, which becomes positive for 'pure' W_2AlC E_{form} (relative to E_{form} of the starting elements), which suggests a metastable character of this phase.[144]

4. Tungsten carbides doped with d-metals

In ternary systems W–M–C(N) (M is a transition metal), both substitution solid solutions $W_xM_yC(N)_z$ retaining the structural type of the starting binary phases (see a review[33]) and ternary phases (see above) with individual chemical composition and structure can form. In this Section, we will consider information on simulation of solid solutions of the general formula $W_xM_yC(N)_z$.

To date, the electronic structures and some properties were studied for $W_{0.75}M_{0.25}C$ (M = Ti, Mo),[148,149] $W_{0.875}M_{0.125}C$ (M = Cr, Co, Zr)[98] and $W_{0.875}M_{0.125}C$ (M is a 3d-metal, such as Sc, Ti, V, ..., Ni, Cu).[150]

A comparative analysis of the energy states of $W_{0.75}M_{0.25}C$ (M = Ti, Mo) with the WC- and NaCl-type structures showed[148] that the introduction of Ti atoms into

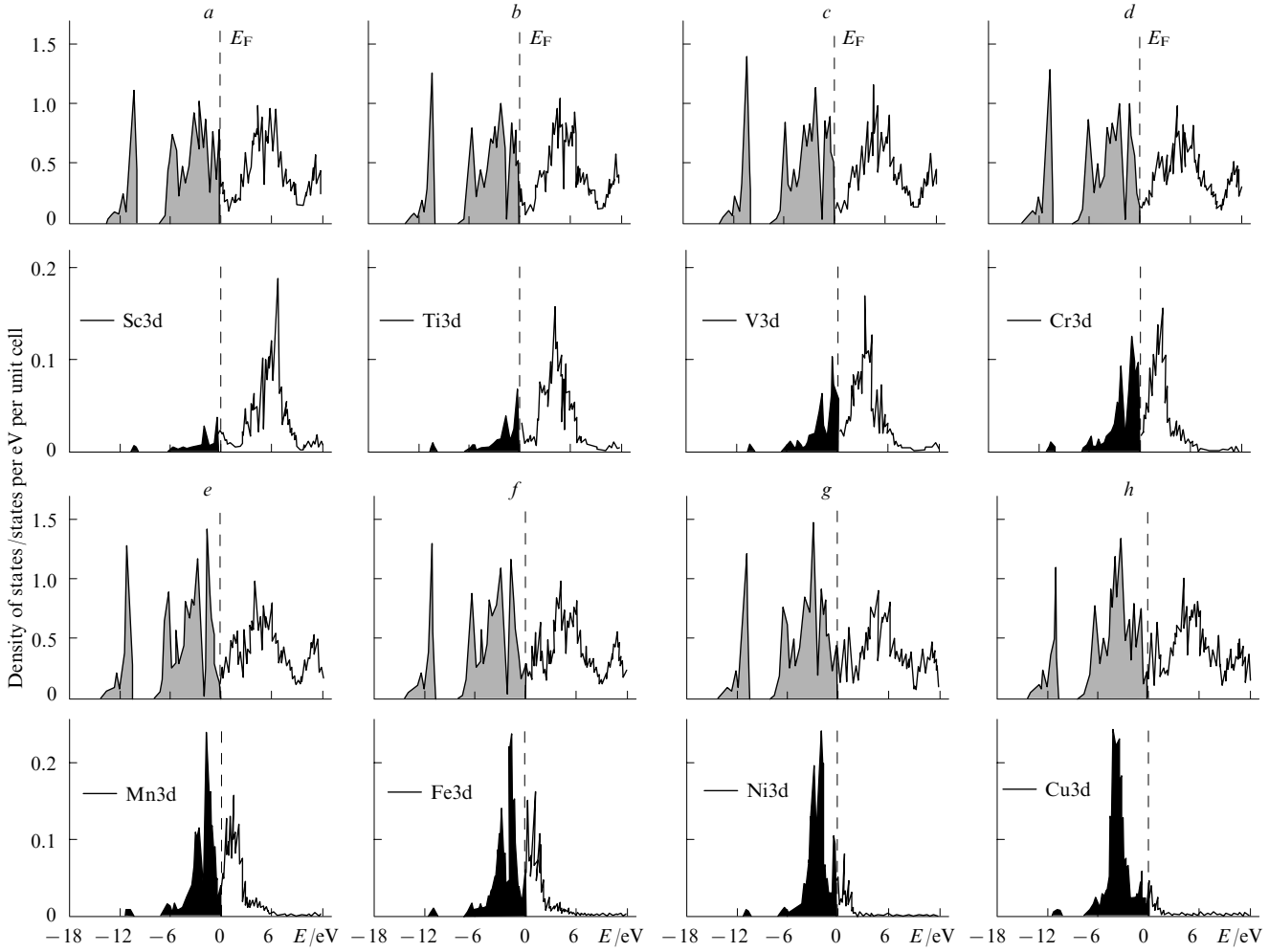


Figure 19. The total and partial densities of states for nonmagnetic ternary solid solutions.[150]
$W_{0.875}Sc_{0.125}C$ (*a*), $W_{0.875}Ti_{0.125}C$ (*b*), $W_{0.875}V_{0.125}C$ (*c*), $W_{0.875}Cr_{0.125}C$ (*d*), $W_{0.875}Mn_{0.125}C$ (*e*), $W_{0.875}Fe_{0.125}C$ (*f*), $W_{0.875}Ni_{0.125}C$ (*g*) and $W_{0.875}Cu_{0.125}C$ (*h*).

Table 9. The total and partial densities of states at the Fermi level, the low-temperature heat capacity coefficients and the Pauli paramagnetic susceptibilities of nonmagnetic solid solutions $W_{0.875}M_{0.125}C$ and h-WC.[150]

System	$N_{tot}(E_F)$	$N^{W5d}(E_F)$	$N^{C2p}(E_F)$	$N^{M3d}(E_F)$	γ /mJ K^{-2} mol^{-1}	χ /10^{-4} emu mol^{-1}
	states per eV per formula unit					
$W_{0.875}Sc_{0.125}C$	0.701	0.215	0.108	0.033	1.66	0.22
$W_{0.875}Ti_{0.125}C$	0.882	0.264	0.115	0.085	2.09	0.27
$W_{0.875}V_{0.125}C$	0.479	0.126	0.066	0.060	1.13	0.15
$W_{0.875}Cr_{0.125}C$	0.294	0.090	0.039	0.043	0.70	0.09
$W_{0.875}Mn_{0.125}C$	0.428	0.176	0.020	0.096	1.01	0.13
$W_{0.875}Fe_{0.125}C$	0.625	0.216	0.049	0.179	1.48	0.19
$W_{0.875}Ni_{0.125}C$	0.362	0.110	0.069	0.058	0.86	0.11
$W_{0.875}Cu_{0.125}C$	0.540	0.171	0.101	0.050	1.28	0.17
h-WC	0.228	0.099	0.029	—	0.54	0.07

tungsten carbide favours stabilization of its cubic polymorph. The authors of Ref. 149 calculated parameters of the electronic spectra of solid solutions $W_{0.875}M_{0.125}C$ (M = Cr, Co, Zr) and evaluated the compression moduli, which appeared to be about 6% – 12% lower than that of binary WC.[149]

Common trends in changes in the electronic spectrum of WC upon partial replacement of tungsten atoms by atoms of 3d-metals (M = Sc, Ti, V, ... , Ni and Cu) were considered.[150] The $W_{0.875}M_{0.125}C$ phases studied (except for $W_{0.875}Co_{0.125}C$) were nonmagnetic systems. The electronic structure of $W_{0.875}M_{0.125}C$ (Fig. 19) is by and large similar to that of tungsten monocarbide (see Section II); the key features of the distribution of states in solid solutions are determined by the positions (and degree of filling) of the valence 3d states of the metal M. On going from Sc to Cu the M3d states are shifted towards the 'interior' of the common valence band of $W_{0.875}M_{0.125}C$ and the degree of filling of these states increases. The concentration of valence electrons in solid solutions increases from 9.625 e per formula unit for $W_{0.875}Sc_{0.125}C$ to 10.625 e per formula unit for $W_{0.875}Cu_{0.125}C$. As a result, the Fermi level is shifted from the top of the hybridized band (W5d + M3d + C2p) to a local minimum of the density of states (see Fig. 19). Noteworthy is a nonmonotonic change in the density of states near E_F (Table 9). On going from Sc to Cu a minimum value of $N(E_F)$ was found for $W_{0.875}Cr_{0.125}C$, which is formed upon isoelectronic substitution W → Cr. The major contribution to the near-E_F region comes from the W5d, M3d and C2p states, the

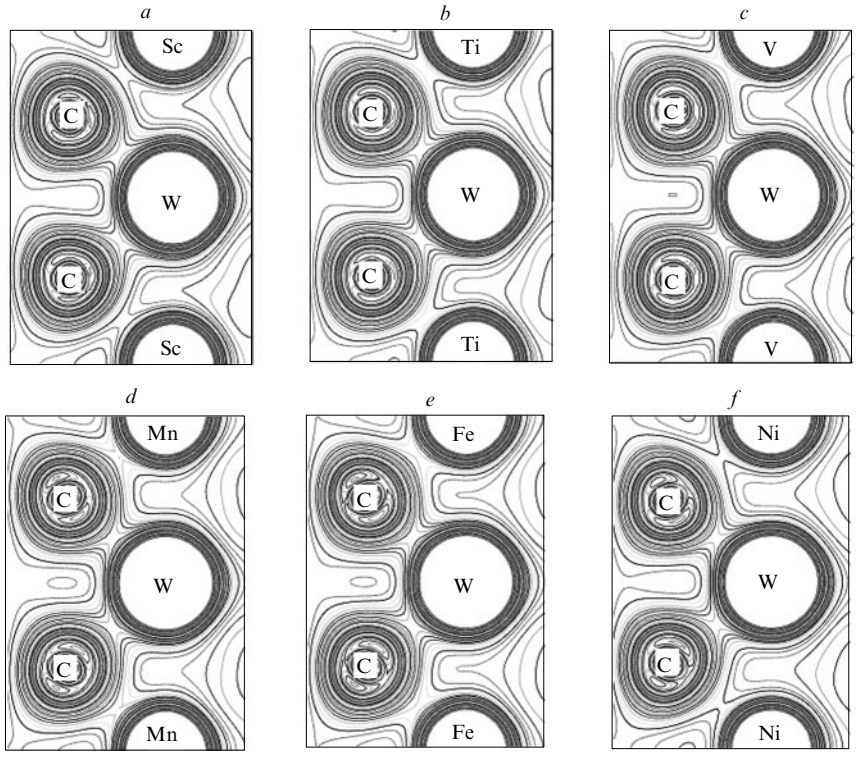


Figure 20. The charge density distributions for the valence states of nonmagnetic ternary solid solutions $W_{0.875}Sc_{0.125}C$ (*a*), $W_{0.875}Ti_{0.125}C$ (*b*), $W_{0.875}V_{0.125}C$ (*c*), $W_{0.875}Mn_{0.125}C$ (*d*), $W_{0.875}Fe_{0.125}C$ (*e*) and $W_{0.875}Ni_{0.125}C$ (*f*).[150]
Isoelectronic contours are drawn with an increment of 0.05 e Å^{-3}.

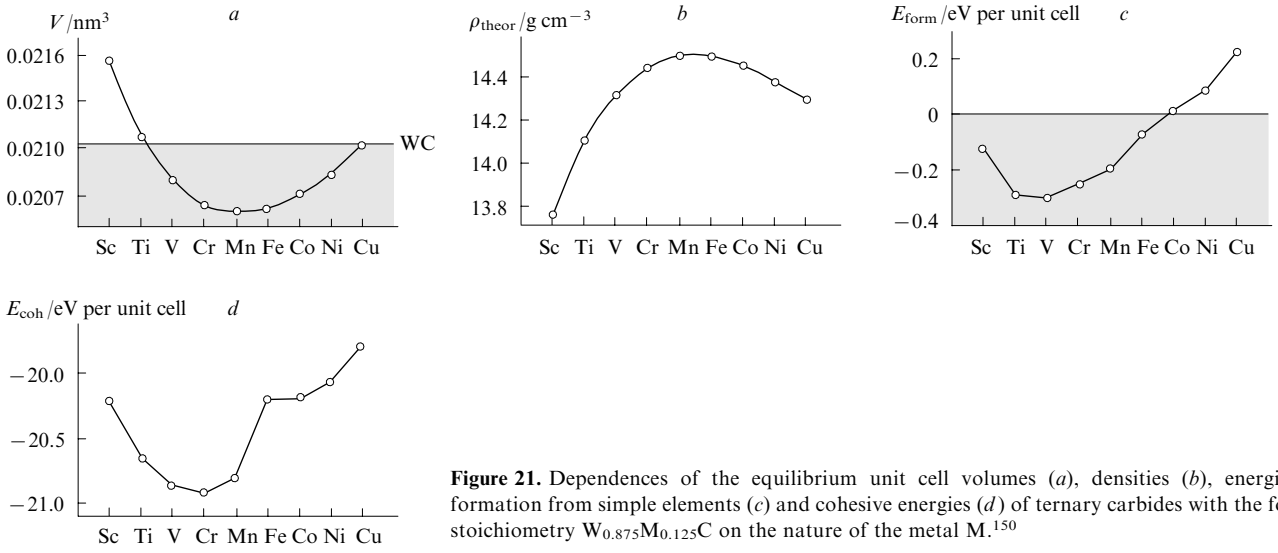


Figure 21. Dependences of the equilibrium unit cell volumes (*a*), densities (*b*), energies of formation from simple elements (*c*) and cohesive energies (*d*) of ternary carbides with the formal stoichiometry $W_{0.875}M_{0.125}C$ on the nature of the metal M.[150]

composition of $N(E_F)$ varies over a rather wide range depending on the type of the 3d impurity.

The evolution of the atom–atom interactions in $W_{0.875}M_{0.125}C$ solid solutions on going from Sc to Cu is illustrated by the charge density maps of the valence states (Fig. 20). The strongest M–C hybrid bonds occur [150] in the solid solutions with the mid-3d row impurities (V, Cr, Mn), whereas the bonds involving M = Sc, Ni, Cu significantly weaken; this is an indirect indication of a greater instability of the systems with M = Sc, Ni, Cu and agrees with the estimates of the energies of formation and cohesive energies (Fig. 21). Analysis of these results showed that:

— for all solid solutions studied one has $|E_{form}(W_{0.875}M_{0.125}C)| < |E_{form}(WC)|$, which indicates a higher stability of tungsten monocarbide, *i.e.*, the introduction of all 3d impurity atoms leads to partial destabilization of the starting tungsten monocarbide;

— for the solid solutions with the early 3d metals one has $E_{form} < 0$, whereas the systems containing the late 3d metals are characterized by $E_{form} > 0$ and are therefore unstable;

— solid solutions $W_{0.875}Co_{0.125}C$ are characterized by nearly zero energies E_{form}; in addition. the most stable solid solution is $W_{0.875}V_{0.875}C$ with partial replacement of W atoms by V.

Of course, a more correct comparison of the data [150] with experimental results requires taking account of the effect of pressure and temperature.

It is noteworthy that for the impurities Sc, Ni and Cu both the energies (E_{form}, E_{coh}) and the calculated [150] equilibrium unit cell volumes (V) and densities (ρ_{theor}) vary nonmonotonically. Eventually, calculations [150] predict that the introduction of cobalt atoms into WC will cause the appearance of local magnetic moments on the Co atoms (0.84 μ_B) due to spin polarization of the Co3d states, whereas the induced magnetic moments of the nearest W and C atoms are very small (< 0.01 μ_B). For $W_{0.875}Co_{0.125}C$, the densities of the spin-'up' and spin-'down' states at the Fermi level differ by about two times, being 0.200 and 0.389 states per eV per formula unit, respectively.

5. Perovskite-like ternary tungsten carbides and nitrides

Among the ternary tungsten-containing carbides and nitrides having individual crystal structures, chemical compositions and properties, there is a group of cubic phases with perovskite-like structure.[151] It includes a ternary carbide W_3NiC, a nitride W_3NiN, which was obtained upon decomposition of metastable Ni_2W_3N,[152] as well as two predicted [151] perovskite-like phases Co_3WC and Rh_3WC.

The electronic, energy, magnetic and mechanical properties Co_3WC, Rh_3WC, Ir_3WC, W_3NiN, and W_3NiC were calculated.[153] One can follow how these properties of perovskite-like tungsten-containing phases vary depending on, first, the type of transition metal (*i.e.*, Co_3WC compared to Rh_3WC); second, the type of the p-element (C or N, *i.e.*, W_3NiC compared to W_3NiN); third, on the W : M ratio (W : M = 3 or M : W = 3, *i.e.*, W_3NiC compared to Co_3WC).

Selected calculated [153] parameters are listed in Table 10. As can be seen, the unit cell volumes of the perovskites decrease in the order

$$V(Ir_3WC) > V(W_3NiC) > V(W_3NiN) > V(Rh_3WC) > > V(Co_3WC),$$

while the densities of the phases increase in the order

$$Co_3WC < Rh_3WC < W_3NiC < W_3NiN < Ir_3WC.$$

All independent elastic constants of the perovskites (C_{11}, C_{12}, C_{44}) are positive and meet the criterion for the mechanical stability of crystals

$$(C_{11} - C_{12}) > 0,$$

$$(C_{11} + 2C_{12}) > 0,$$

$$C_{44} > 0.$$

The compression moduli are rather close (they are in the interval ~256–297 GPa), being much lower than those of the binary tungsten carbides ($B \approx 384$ GPa for h-WC and $B \approx 363$ GPa for c-WC).[85] For all antiperovskite phases one has $B > G$, which means that the parameter limiting the stability of these crystals is the shear modulus. In addition, the calculated elastic constants allow one to estimate the so-called Pugh criterion [97] ($P = G/B$) and the Cauchy pres-

Table 10. Optimized lattice constants and the energy, magnetic and mechanical properties of perovskite-like tungsten-containing phases.[153]

Parameter	W_3NiC	W_3NiN	Co_3WC	Rh_3WC	Ir_3WC
a /nm	0.4092	0.4064	0.3808	0.4060	0.4095
V /nm^3	0.0685	0.0671	0.0552	0.0669	0.0687
ρ_{theor} /g cm^{-3}	15.077	15.447	11.250	12.519	18.687
$-E_{coh}$ /eV per formula unit	49.10	49.54	36.20	40.01	46.48
$-E_{form}$ /eV per formula unit	1.33	–	1.25	0.98	2.36
C_{11} /GPa	498	606	437	387	355
C_{12} /GPa	159	143	167	191	207
C_{44} /GPa	106	78	87	51	17
B /GPa	272	297	257	256	256
G /GPa	131	139	106	70	40
$N^{W5d}(E_F)$ [a]	1.521	1.236	0.612 0.061	0.517 0.288	1.176 0.526
$N^{Md}(E_F)$ [a]	0.690	0.649	0.972 2.145	1.147 0.563	1.759 0.669
$N(E_F)$ [a]	3.908	3.228	2.398 2.460	2.557 1.494	4.603 2.202
γ /mJ K^{-2} mol^{-1}	9.26	7.65	–	–	–
χ /10^{-4} emu mol^{-1}	1.20	0.99	–	–	–

Note. For the magnetic phases, listed are the densities of the spin-'up' (numbers in the numerator) and spin-'down' states (numbers in the denominator). [a] Given in states per eV per formula unit.

sure[88] ($CP = C_{12} - C_{44}$). For all antiperovskites one has $CP > 0$ and $G/B < 0.5$; thus, according to the known rules,[88, 97, 154, 155] all these phases belong to plastic materials with metal-like type of chemical bonding.

The stability of all perovskite-like phases was evaluated from their cohesive energies. For the carbides, the energies of their formation relative to metals (W, Ni, Co, Rh, Ir) and graphite were also calculated. It was found that the E_{coh} values decrease in the following order

$$W_3NiN \rightarrow W_3NiC \rightarrow Ir_3WC \rightarrow Rh_3WC \rightarrow Co_3WC,$$

and all cohesive energies of ternary phases are lower in absolute value than that of WC. Interestingly, for the ternary phases one has

$$E_{coh}(W_3NiN) < E_{coh}(W_3NiC),$$

while for the binary phases one gets[85]

$$E_{coh}(WC) < E_{coh}(WN).$$

This can be due to strengthening of metallic character of the Ni–W bond with shortening of the distance between Ni and W atoms on going from W_3NiC to W_3NiN.[153] The energies of formation of ternary carbides are positive, which means that these phases are metastable relative to mechanical mixtures of simple reactants.

Electronic structure calculations showed that W_3NiC and W_3NiN are nonmagnetic phases. The valence band of W_3NiC is composed of three main bands (peaks *A*, *B*, *C*, Fig. 22). The low-energy band *A* is composed of C(N)2s

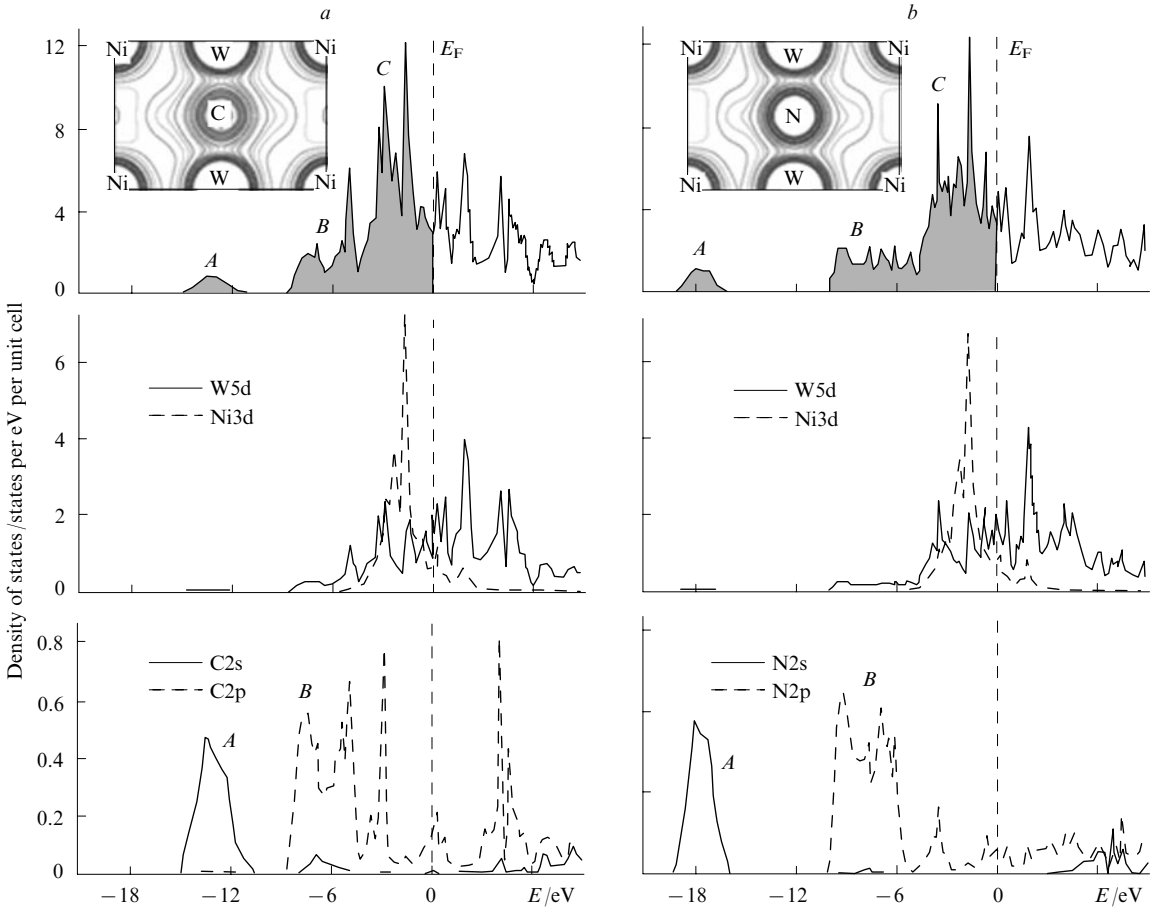


Figure 22. The total and partial densities of states for nonmagnetic perovskite-like phases W_3NiC (*a*) and W_3NiN (*b*).[153]
Insets: charge density maps for the valence states in the (110) plane. Isoelectronic contours are drawn with an increment of 0.05 e Å^{-3}.

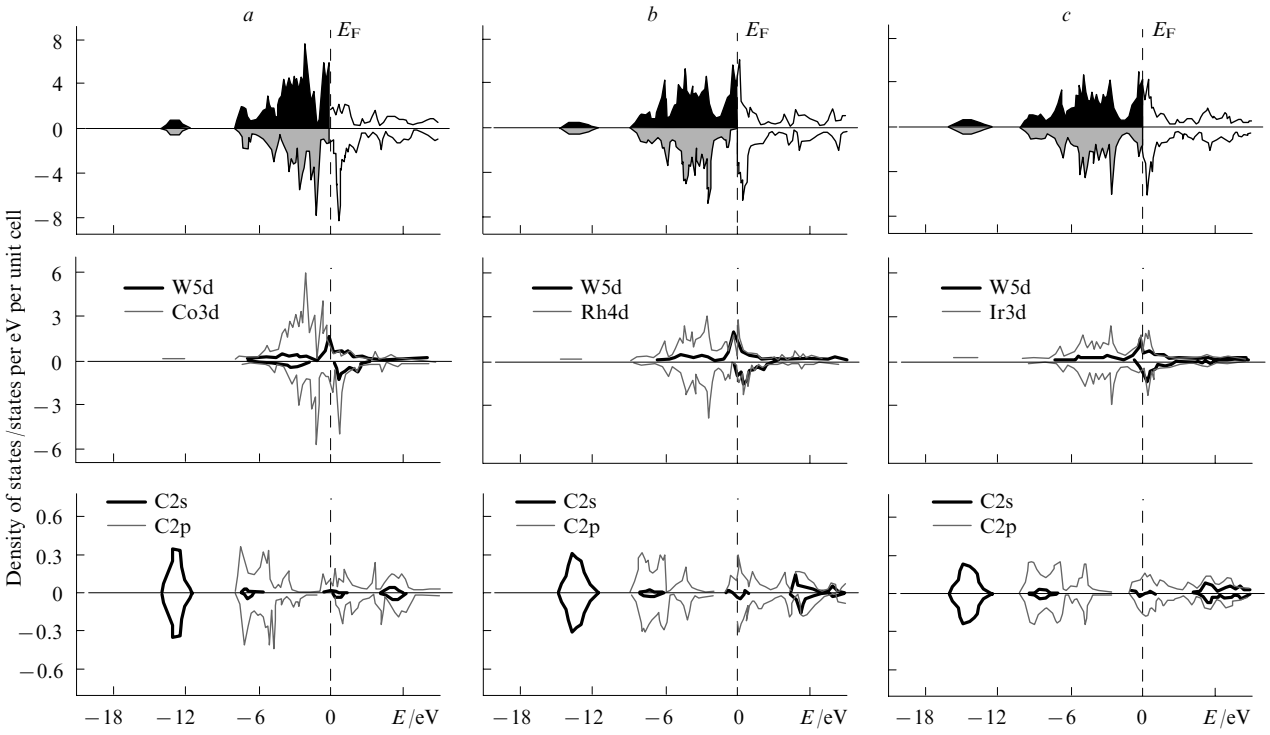


Figure 23. The total and partial spin densities of electronic states for magnetic perovskite-like phases Co_3WC (*a*), Rh_3WC (*b*) and Ir_3WC (*c*).

states and separated from the next band *B*, which is mainly formed by the C(N)2p states (with mixing of W5d and Ni3d states), by a gap of about 1.8 eV. The third band *C* (near E_F) is mainly filled with the W5d and Ni3d states.

Interatomic interactions in W_3NiC and W_3NiN are of a complex character and include a metallic component (due to delocalized W5d and Ni3d states) corresponding to the band *C* and an ionic component determined by transfer of the charge density from the transition metal to carbon (nitrogen) atoms. The covalent bond is formed by the overlapping C(N)2p and W5d states, as is clearly seen in the charge density maps (see Fig. 22). These maps also show weakening of metal–nonmetal covalent bonds on going from W_3NiC to W_3NiN.

Unlike W_3NiC and W_3NiN, the phases Co_3WC, Rh_3WC and Ir_3WC are magnetic in the ground state (Fig. 23). The onset of magnetism is due to spin polarization of both metal sublattices (Co, Rh or Ir and tungsten); the corresponding atomic magnetic moments are listed in Table 11. As can be seen, the total magnetic moments (calculated per unit cell) considerably decrease in the order $Co_3WC \rightarrow Rh_3WC \rightarrow Ir_3WC$. In addition, for Co_3WC the major contribution to the total magnetic moment comes from the cobalt atomic moments (Fig. 24). The reverse is observed for Rh_3WC and Ir_3WC, *viz.*, the magnetization of these phases is governed

Table 11. The total magnetic moments (per unit cell) and atomic magnetic moments (μ_B) in antiperovskites Co_3WC, Rh_3WC, Ir_3WC.[153]

Phase	μ_{tot}	μ^W	$\mu^{Co,\ Rh,\ Ir}$	μ^C
Co_3WC	4.10	0.46	1.10	0.01
Rh_3WC	2.81	1.23	0.18	0.10
Ir_3WC	1.50	0.69	0.08	0.02

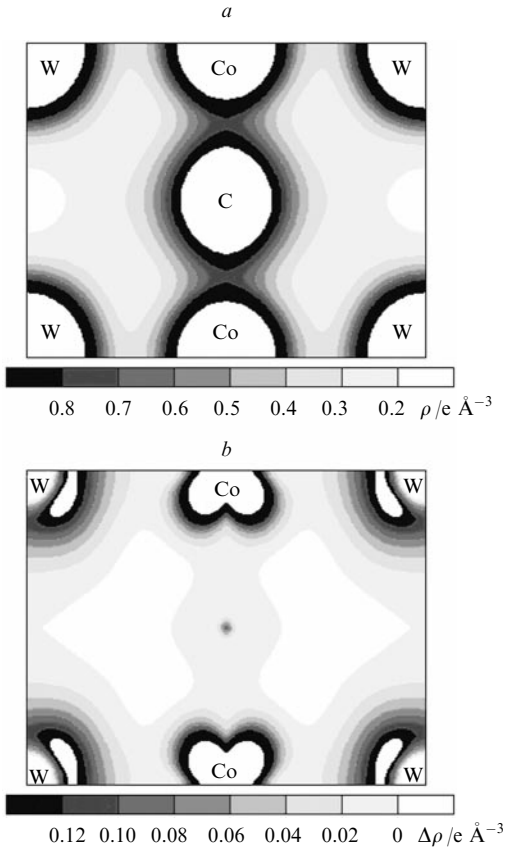


Figure 24. The charge density maps for the valence states (*a*) and differene spin density ($\Delta\rho = \rho_\uparrow - \rho_\downarrow$) (*b*) in antiperovskite Co_3WC in the (110) plane.[153]

by the magnetic moments of atoms in the tungsten sublattice (see Table 11).

6. Tungsten-containing η-phases

Among ternary tungsten-containing carbides, there is a group of η-phases which are formed in composites in the space between WC grains and transition metals (M) or their alloys. As the so-called secondary phases, they significantly affect the properties (*e.g.*, mechanical ones) of these tungsten-containing materials [156–163] similarly to the effect of Cr_7C_3 phases, cementite (Fe_3C) or Fe_2B on the properties of the carbon or Fe–B-steels and cast irons.[164–167]

Among tungsten-containing η-phases with different M : W ratio (*e.g.*, Co_2W_4C or Co_4W_2C), [33] the most widely known are η-carbides with the stoichiometry M : W = 1, namely, M_3W_3C and M_6W_6C.[156–163, 168–174] Synthetic routes to the η-phases include, *e.g.*, mechanochemical treatment of corresponding binary carbides.[168–170] η-Carbides possess a number of interesting properties. For instance, the compression modulus B of Co_6W_6C is 462 GPa,[175] being higher than those of diamond (∼ 444 GPa) and h-WC (∼ 421 GPa); Fe_3W_3C and Fe_6W_6C exhibit a rather high microhardness ($H_V \approx 15.6$ GPa).[170]

According to the available crystallographic data,[3, 176–178] η-carbides have a cubic structure (space group $Fd3m$) with $Z = 16$ (for M_3W_3C) and $Z = 8$ (for M_6W_6C). In the M_3W_3C and M_6W_6C lattices, tungsten atoms occupy the positions 48*f*, the atoms M occupy two nonequivalent positions 32*e* (M_1) and 16*d* (M_2) and carbon atoms occupy the positions 16*c* (for M_3W_3C) or 8*a* (for M_6W_6C) (Fig. 25).

Recently, detailed *ab initio* studies of the electronic structure, atom–atom interactions and some structural, mechanical, cohesive and magnetic properties of η-carbides M_3W_3C (M = Fe, Co, Ni) and M_6W_6C (M = Fe, Co) were carried out for the first time.[179–181] The structural data thus obtained (Table 12), in particular, show that

$$a(Fe_3W_3C) > a(Fe_6W_6C),$$

$$a(Co_3W_3C) > a(Co_6W_6C).$$

The theoretical density decreases in the order

$$Co_6W_6C > Fe_6W_6C > Co_3W_3C > Fe_3W_3C,$$

Table 12. Lattice constants, theoretical densities, uniform compression moduli and shear moduli of cubic η-carbides M_3W_3C and M_6W_6C (M = Fe, Co, Ni).

η-Carbide	a /nm	ρ_{theor} /g cm^{-3}	B /GPa	G /GPa	Ref.
Fe_3W_3C	1.1032	14.464	–	–	180
	1.1087	–	–	–	117
	1.084	–	371.2	182.2	181
Co_3W_3C	1.1023	14.685	–	–	180
	1.1112	–	–	–	176
	1.088	–	351.1	158.1	181
Ni_3W_3C	1.17	–	–	–	182
	1.090	–	331.2	143.3	181
Fe_6W_6C	1.0900	14.873	–	–	180
	1.090	–	–	–	178
Co_6W_6C	1.0877	15.163	–	–	180
	1.0897	–	–	–	176

i.e., the Co-containing phases have a higher density than the Fe-containing phases (with the same (W, M) : C ratio).[180] In addition, one has $\rho_{theor}(M_6W_6C) > \rho_{theor}(M_3W_3C)$, *i.e.*, the phases with lower carbon content are more dense. At the same time, for all ternary carbides M_3W_3C and M_6W_6C the ρ_{theor} values are lower than the theoretical density of h-WC (about 15.40 g cm^{-3}).

Estimates [181] of the compression and shear moduli of the M_3W_3C phases showed that these parameters decrease (see Table 12) in the order

$$Fe_3W_3C > Co_3W_3C > Ni_3W_3C.$$

Taking into account the known correlations between the B and G moduli and the hardness, Fe_3W_3C is expected to be the hardest among the M_3W_3C phases.[181] This phase is also characterized by the lowest compressibility, which ranks the second after that of diamond (Fig. 26).

The energies of formation of the M_3W_3C phases calculated relative to the corresponding metals and graphite decrease in absolute value as follows:[181]

$$Fe_3W_3C > Co_3W_3C > Ni_3W_3C.$$

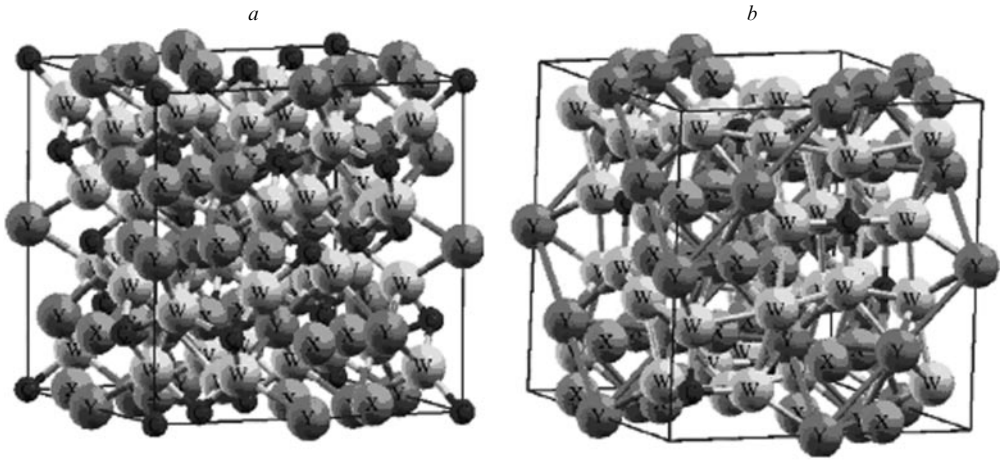


Figure 25. Fragments of the crystal structures of M_3W_3C (*a*) and M_6W_6C (*b*) (M = Co, Fe).
X and Y are two types of nonequivalent 3d-metal atoms occupying the positions 32*e* and 16*d*.

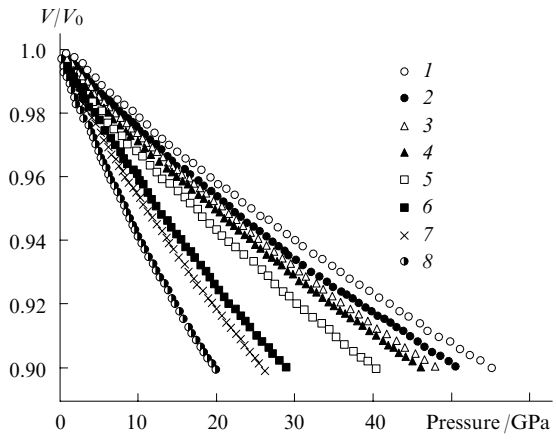


Figure 26. Compressibilities of the phases M_3W_3C (M = Fe, Co, Ni) and other materials.[181]
Diamond (*1*), Fe_3W_3C (*2*), Co_3W_3C (*3*), Ni_3W_3C (*4*), Fe_3C (*5*), Cr_7C_3 (*6*), Fe_2B (*7*) and Cu (*8*).

According to E_{form} calculations for the η-carbides M_3W_3C and M_6W_6C,[180] the most stable is Fe_6W_6C, whereas Co_3W_3C is the least stable. At the same time, all η-phases are less stable than h-WC, which is in good agreement with experimental data; namely, sintering of mixtures of elemental reactants in the ternary systems (Fe,Co)–W–C results in primary products [mainly WC and Fe(Co)], while η-carbides are formed as intermediate phases only after subsequent activation (grinding, heating, *etc.*).[157, 160, 183, 184] An attempt[180] to estimate the energies of formation of η-carbides in the reactions involving h-WC and the most stable phase of tungsten subcarbide (ε-W_2C) showed that in the former case one gets $E_{form} > 0$ and thus the latter case is energetically more favourable.

Analysis of the magnetic and electronic properties of the η-phases showed[180] that Co_3W_3C and Co_6W_6C are nonmagnetic in the ground state, whereas the Fe-containing carbides mainly possess the properties of ferromagnetics. However, the energy gain in the latter case is small compared to nonmagnetic, being about 0.001 eV per atom for Fe_3W_3C and 0.002 eV per atom for Fe_6W_6C.

The total and partial densities of states of nonmagnetic Co_3W_3C and Co_6W_6C are shown in Fig. 27. The spectra of these phases exhibit a number of common features. For instance, in both spectra the low-energy band (peak *A*) is composed of C2s states. The filled (W + Co)d bands are localized in the interval from −8.2 eV to E_F (for Co_3W_3C) and from −8.4 eV to E_F (for Co_6W_6C); these states are separated from the C2s states by forbidden gaps of about 3.6 and 3.7 eV, respectively. Emphasize that the Co3d band is much narrower than the W5d band (these bands overlap with each other). As a result, the bottom of the valence band

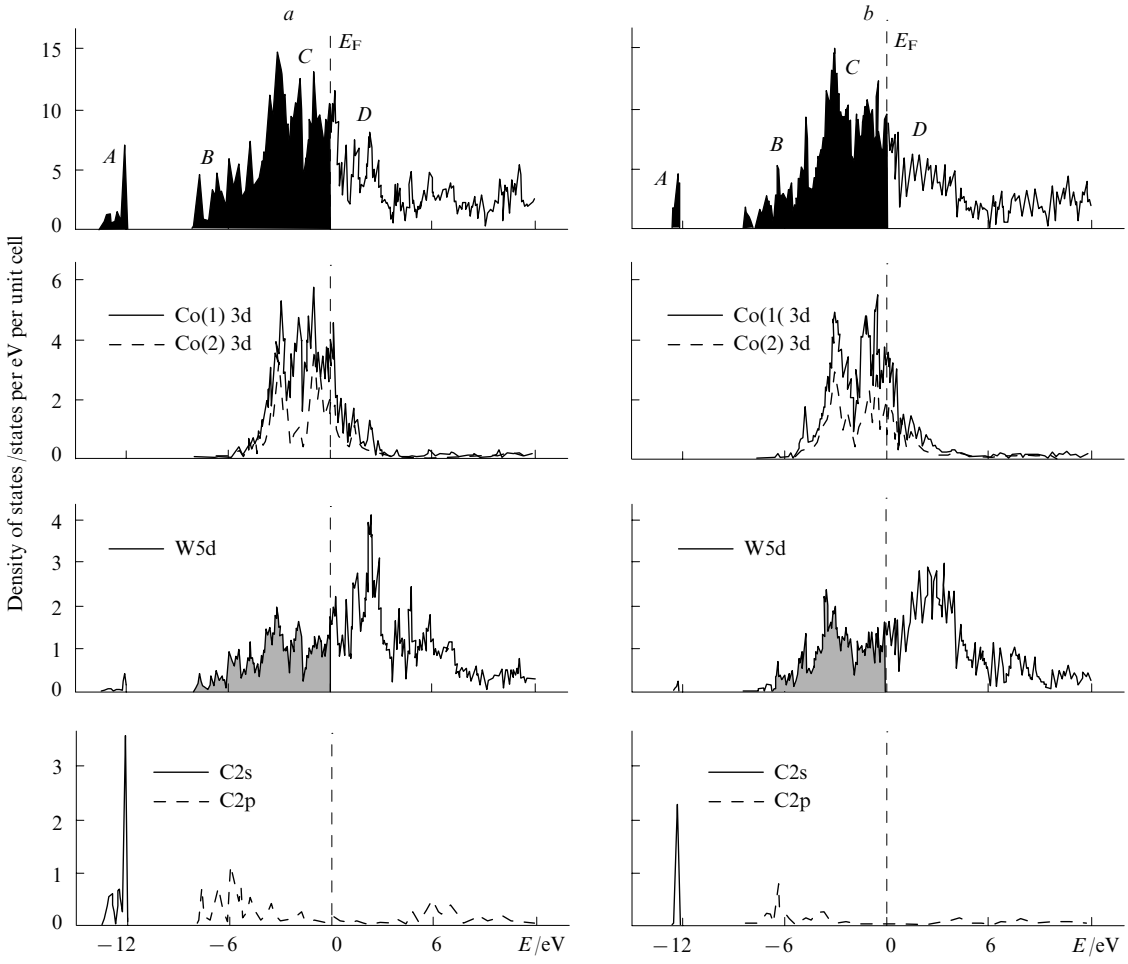


Figure 27. The total and partial densities of states for ternary η-carbides Co_3W_3C (*a*) and Co_6W_6C (*b*).[180]

(peak *B*) is formed by the W5d states, which overlap with the C2p states and form covalent bonds W–C. The Co3d–C2p overlap is much weaker. The upper part of the valence band and the bottom of the conduction band (peaks *C* and *D*) have a (W + Co)d mixed character and the Fermi level is in the region of the peaks *C* and *D*. The $N(E_F)$ values decrease (in the nonmagnetic state) as follows:

$$Fe_6W_6C > Fe_3W_3C > Co_6W_6C > Co_3W_3C,$$

i.e., the Fe-containing phases in the nonmagnetic state are characterized by higher $N(E_F)$ values compared to the Co-containing phases. This provides a qualitative explanation for the nonmagnetic state of the Co-containing η-carbides. On going from M_3W_3C to M_6W_6C (as the concentration of carbon atoms decreases), the $N(E_F)$ values increase. An analysis of the orbital contributions to $N(E_F)$ showed[180] that the W5d and (Co,Fe)3d states give comparable contributions to the near-E_F region, whereas the contribution of the C2p states is small. For the ferromagnetic carbides Fe_3W_3C and Fe_6W_6C, a spin splitting of the Fe3d states was found. The magnetic moments of iron atoms vary from 0.10 to 0.75 μ_B depending on the type of positions; the induced magnetic moments of tungsten and carbon atoms are very small.

As in other tungsten-containing phases considered in the review, chemical bonds in η-carbides are of mixed character.[180, 181] Covalent bonds are formed by the W5d–C2p hybridized orbitals, the formation of ionic bonds is due to partial transfer of the electron density from the metal to carbon atoms. The metallic component is due to mixing of delocalized d states of the atoms of W and 3d-metals containing in the η-phases. The populations of particular (pair) bonds (*n*, e) in these materials are comparable. For instance, for Fe_3W_3C one has $n(W-C) = 0.35$, $n(Fe-W) = 0.23$, $n(W-W) = 0.13$ and $n(Fe-Fe) = 0.10$.[181]

V. Conclusion

Summing up, considerable progress has recently been made in the interpretation and prediction of many properties of tungsten-containing compounds using *ab initio* computational methods of quantum chemistry and computer-assisted materials science.

In the early stage of investigations (1970s–1990s) the emphasis was mainly placed on the electronic spectra of the simplest highly symmetric perfect crystals (WC and WN). At present, theoretical studies concern much more complex systems (solid solutions of variable composition, ternary phases of complex structure and chemical compositions, *e.g.*, η-carbides, *etc.*) for which not only parameters of the electronic spectra are determined, but also microscopic analysis and prediction of a rather large number of physicochemical properties including structural, cohesive, mechanical, magnetic ones, *etc.*, is made. This is of great importance for progress in fundamentals of materials science of tungsten-containing systems.

At the same time, many issues in theoretical materials science of these systems are still to be solved. We believe they include the effect of lattice defects on the physicochemical properties of these materials, systematic investigations on the peculiar features of their surface states and interfaces for heterogeneous systems involving tungsten carbides and nitrides. At present, there are only a few studies on the theoretical description of the effect of vacancies in the tungsten and carbon sublattices on the properties of WC (Refs 82 and 83) and on consideration of specific features of the surface electronic states of monocarbide WC (Refs 74 and 99) and interfacial regions in WC/Co,[183, 184] WC/HfO_2,[185] WC/Al (Ref. 99) and WC/C composites.[186]

Simulations of the morphologies, electronic structure and properties of the available (already synthesized) tungsten carbides and nitrides and related tungsten-containing systems in the nano state (in the form of nanopowders, nanofilaments, nanotubes and nanocomposites) are scarce. Taking into account the potential of modern *ab initio* methods and a great experience in using them to simulate various nanoforms of carbides and nitrides of other transition metals,[16–30] one can expect that corresponding investigations of tungsten-containing nanomaterials will be set in the nearest future.

The review has been written with the financial support from the Russian Foundation for Basic Research (Project No. 08-08-00034).

References

1. H J Goldschmidt *Interstitial Alloys* (London: Butterworths, 1967)
2. E K Storms *The Refractory Carbides* (New York: Academic Press, 1967)
3. L Toth *Transition Metal Carbides and Nitrides* (New York: Academic Press, 1971)
4. G V Samsonov, G Sh Upadkhaya, V S Neshpor *Fizicheskoe Materialovedenie Karbidov* (Physical Materials Science of Carbides) (Kiev: Naukova Dumka, 1974)
5. G V Samsonov, I M Vinnitskii *Tugoplavkie Soedineniya* (Refractory Compounds) (Moscow: Metallurgiya, 1976)
6. G P Shveikin S I Alyamovskii, Yu G Zainulin, A I Gusev, V A Gubanov, E Z Kurmaev *Soedineniya Peremennogo Sostava i ikh Tverdye Rastvory* (Compounds of Variable Composition and Their Solid Solutions) (Sverdlovsk: Ural Scientific Centre, Academy of Sciences of USSR, 1984)
7. *Svoistva, Poluchenie i Primenenie Tugoplavkikh Soedinenii (Spravochnik)* [Properties, Production and Application of Refractory Compounds) (Handbook)] (Ed. T Ya Kosolapova) (Kiev: Naukova Dumka, 1986)
8. *The Physics and Chemistry of Carbides, Nitrides and Borides (NATO ASI Ser. E)* Vol. 185 (Ed. R Freer) (Dordrecht: Kluwer Academic, 1990)
9. *The Chemistry of Transition Metal Carbides and Nitrides*. (Ed. S T Oyama) (London: Blacklie Academic and Professional, 1996)
10. A L Ivanovskii, V P Zhukov, V A Gubanov *Elektronnoe Stroenie Tugoplavkikh Karbidov i Nitridov Perekhodnykh Metallov* (Electronic Structure of Refractory Carbides and Nitrides of Transition Metals) (Moscow: Nauka, 1990)
11. A L Ivanovskii, A I Gusev, G P Shveikin *Kvantovaya Khimiya v Materialovedenii. Troinye Karbidy i Nitridy Perekhodnykh Metallov i Elementov IIIb, IVb Podgrupp* (Quantum Chemistry in Materials Science. Ternary Carbides and Nitrides of Transition Metals and Elements of Groups IIIb, IVb) (Ekaterinburg: Ural Branch of the Russian Academy of Sciences, 1996)
12. V M Cherkashenko, S Z Nazarova, A I Gusev, A L Ivanovskii *Zh. Strukt. Khim.* **42** 1196 (2001) [a]
13. A I Gusev *Nanokristallicheskie Materialy: Metody Polucheniya i Svoistva* (Nanocrystalline Materials: Methods of Production and Properties) (Ekaterinburg: Ural Branch of the Russian Academy of Sciences, 1998)
14. R A Andrievski *Usp. Khim.* **74** 1163 (2005) [*Russ. Chem. Rev.* **74** 1061 (2005)]
15. A I Gusev *Nanomaterialy, Nanostruktury, Nanotekhnologii* (Nanomaterials, Nanostructures, Nanotechnologies) (Moscow: Fizmatlit-Nauka, 2005)

16. A L Ivanovskii *Teor. Eksp. Khim.* **43** 1 (2007) [b]
17. Yu N Makurin, A A Sofronov, A I Gusev, A L Ivanovsky *Chem. Phys.* **270** 293 (2001)
18. A L Ivanovskii, M V Ryzhkov, V V Ivanovskaya, A A Sofronov, Yu N Makurin, G P Shveikin *Dokl. Akad. Nauk* **378** 68 (2001) [c]
19. A L Ivanovskii, A A Sofronov, Yu N Makurin *Mendeleev Commun.* 59 (2001)
20. V V Ivanovskaya, A A Sofronov, A L Ivanovskii *Zh. Strukt. Khim.* **42** 820 (2001) [a]
21. A A Sofronov, V V Ivanovskaya, Yu N Makurin, A L Ivanovskii *Chem. Phys. Lett.* **351** 35 (2002)
22. V V Ivanovskaya, A A Sofronov, A L Ivanovskii *Phys. Lett. A* **297** 436 (2002)
23. V V Ivanovskaya, A A Sofronov, Yu N Makurin, A L Ivanovskii *J. Mol. Struct. (THEOCHEM)* **594** 31 (2002)
24. A N Enyashin, A L Ivanovskii *Physica E* **30** 164 (2005)
25. A N Enyashin, V G Bamburov, A L Ivanovskii *Dokl. Akad. Nauk* **407** 53 (2006) [c]
26. A N Enyashin, A L Ivanovskii *Zh. Strukt. Khim.* **47** 568 (2006) [a]
27. V V Ivanovskaya, Ch Köhler, G Seifert *Phys. Rev. B* **75** 075410 (2007)
28. A N Enyashin, A L Ivanovskii *Pis'ma Zh. Eksp. Teor. Fiz.* **86** 609 (2007) [d]
29. A N Enyashin, A L Ivanovskii *Mater. Lett.* **62** 662 (2008)
30. V V Ivanovskaya, A L Ivanovskii *Nanostruktury. Matem. Fiz. Modelir.* **1** 7 (2009)
31. A N Enyashin, A L Ivanovskii *Chem. Phys.* **362** 58 (2009)
32. G V Samsonov, V K Vitryanyuk, F I Chaplygin *Karbidy Vol'frama* (Carbides of Tungsten) (Kiev: Naukova Dumka, 1974)
33. A S Kurlov, A I Gusev *Usp. Khim.* **75** 687 (2006) [*Russ. Chem. Rev.* **75** 617 (2006)]
34. L Gao, B H Kear *Nanostruct. Mater.* **9** 205 (1997)
35. P Aratd, L Bartha, R Porat, S Berger, A Rosen *Nanostruct. Mater.* **10** 245 (1998)
36. H H Nersisyan, H I Won, C W Won, J H Lee *Mater. Chem. Phys.* **94** 153 (2005)
37. A S Kurlov, S Z Nazarova, A I Gusev *Pis'ma Zh. Eksp. Teor. Fiz.* **82** 509 (2005) [d]
38. S J Wang, C H Chen, S C Chang, C H Wong, K M Uang, T M Chen, R M Ko, B W Liou *Nanotechnology* **16** 273 (2005)
39. S Shanmugam, D S Jacob, A Gedanken *J. Phys. Chem. B* **109** 19056 (2005)
40. S V Pol, V G Pol, A Gedanken *Adv. Mater.* **18** 2023 (2006)
41. N Keller, B Pietruszka, V Keller *Mater. Lett.* **60** 1774 (2006)
42. G L Tan, X J Wu, Z Q Li *Adv. Eng. Mater.* **8** 62 (2006)
43. A L Ivanovskii *Usp. Khim.* **78** 328 (2009) [*Russ. Chem. Rev.* **78** 303 (2009)]
44. E Gregoryanz, C Sanloup, M Somayazulu, J Badro, G Fiquet, H K Mao, R L Hemley *Nat. Mater.* **3** 294 (2004)
45. J C Crowhurst, A F Goncharov, B Sadigh, C L Evans, P G Morrall, J L Ferreira, A J Nelson *Science* **311** 1275 (2006)
46. A F Young, C Sanloup, E Gregoryanz, S Scandolo, R J Hemley, H K Mao *Phys. Rev. Lett.* **96** 155501 (2006)
47. *The Properties of Natural and Synthetic Diamond* (Ed. J E Field) (London: Academic Press, 1992)
48. *The Nature of Diamonds* (Ed. E G Harlow) (New York: Cambridge University Press, 1998)
49. V V Brazhkin *High Pres. Res.* **27** 333 (2007)
50. J J Gilman, R W Cumberland, R B Kaner *Int. J. Refract. Met. Hard Mater.* **24** 1 (2006)
51. P Kroll, T Schroter, M Peters *Angew. Chem., Int. Ed.* **44** 4249 (2005)
52. H Wang, Q Li, Y Li, Y Xu, T Cui, A R Oganov, Y Ma *Phys. Rev. B* **79** 132109 (2009)
53. A Klimpel, L A Dobrzanski, A Lisiecki, D Janicki *J. Mater. Proc. Technol.* **164** 1068 (2005)
54. T Li, Q Li, J Fuh, P Yu, C Wu *Mater. Sci. Eng. A* **430** 113 (2006)
55. J Iwaszko, Z Nitkiewicz *Mater. Manufact. Proc.* **17** 169 (2002)
56. T Li, Q Lou, J Dong, Y Wei, J Liu *Appl. Phys. A* **73** 391 (2001)
57. M F Morks, Y Gao, N F Fahim, F U Yinquing *Mater. Lett.* **60** 1049 (2009)
58. M K Neylon, S Choi, H Kwon, K E Curry, L T Thompson *Appl. Catal., A* **183** 253 (1999)
59. H Meng, M Wu, X Hu, M Nie, Z Wei, P Shen *Fuel Cells* **6** 447 (2006)
60. Y Ishikawa, H Jinbo, H Yamanaka *Jpn. J. Appl. Phys.* **45** L50 (2006)
61. A I Gusev, A S Kurlov *Pis'ma Zh. Eksp. Teor. Fiz.* **85** 34 (2007) [d]
62. T Iizuka, H Kita, T Hirai, K Osumu *Wear* **257** 953 (2004)
63. C Liang, F Tian, Z Li, Z Feng, Z Wei, C Li *Chem. Mater.* **15** 4846 (2003)
64. C Liang, F Tian, Z Wei, Q Xin, C Li *Nanotechnology* **14** 955 (2003)
65. J Yan, X Ma, W Zhao, H Tang, C Zhu, S Cai *Mater. Res. Bull.* **40** 701 (2005)
66. J Yan, X Ma, W Zhao, H Tang, C Zhu, S Cai *Metall. Mater. Trans. A* **37** 1692 (2006)
67. J Yan, X Ma, W Zhao, H Tang, C Zhu, S Cai *Int. J. Refract. Met. Hard Mater.* **25** 62 (2007)
68. H Tang, X Ma, W Zhao, X Yan, J Yan *Mater. Res. Bull.* **39** 707 (2004)
69. J Yan, X Ma, W Zhao, H Tang, C Zhu, S Cai *Mater. Sci. Eng. B* **117** 321 (2005)
70. J Yan, X Ma, W Zhao, H Tang, C Zhu *J. Solid State Chem.* **177** 2265 (2004)
71. D V Suetin, I R Shein, A S Kurlov, A I Gusev, A L Ivanovskii *Fiz. Tv. Tela* **50** 1366 (2008) [e]
72. D V Suetin, I R Shein, A L Ivanovskii *J. Phys. Chem. Solids* **70** 64 (2009)
73. E S Alekseev, P G Arkhipov, S V Popova *Phys. Status Solidi B* **110** K151 (1982)
74. L F Mattheiss, D R Hamann *Phys. Rev. B* **30** 1731 (1984)
75. V P Zhukov, V A Gubanov *Solid State Commun.* **56** 51 (1985)
76. V P Zhukov, V A Gubanov, T Jarlborg *J. Phys. Chem. Solids* **46** 1111 (1985)
77. V P Zhukov, V A Gubanov *Izv. Akad. Nauk SSSR, Neorg. Mater.* **22** 1665 (1986) [f]
78. A Y Liu, R M Wentzcovitch, M L Cohen *Phys. Rev. B* **38** 9483 (1988)
79. A Y Liu, M L Cohen *Solid State Commun.* **67** 907 (1988)
80. D L Price, B R Cooper *Phys. Rev. B* **39** 4945 (1989)
81. M Rajagopalan, P Saigeetha, G Kalpan *Jpn. J. Appl. Phys.* **33** 1847 (1994)
82. A L Ivanovskii, N I Medvedeva *Mendeleev Commun.* 10 (2001)
83. N I Medvedeva, A L Ivanovskii *Fiz. Tv. Tela* **43** 469 (2001) [e]
84. E I Isaev, S I Simak, I A Abrikosov, R Ahuja, Yu Kh Vekilov, M I Katsnelson, A I Lichtenstein, B Johansson *J. Appl. Phys.* **101** 123519 (2007)
85. D V Suetin, I R Shein, A L Ivanovskii *Phys. Stat. Solidi B* **245** 1590 (2008)
86. I R Shein, D V Suetin, A L Ivanovskii *Pis'ma Zh. Tekh. Fiz.* **34** 53 (2008) [g]
87. A H Cottrell *Mater. Sci. Technol.* **11** 209 (1995)
88. J F Nye *Physical Properties of Crystals* (Oxford: Oxford University Press, 1985)
89. Ch Kittel *Introduction to Solid State Physics* (Berkeley, CA: University of California, 2005)
90. I R Shein, V S Kiiko, Yu N Makurin, M A Gorbunova, A L Ivanovskii *Fiz. Tv. Tela* **49** 1015 (2007) [e]
91. I R Shein, K I Shein, A L Ivanovskii *Pis'ma Zh. Tekh. Fiz.* **33** 72 (2007) [g]
92. M Lee, R S Gilmore *J. Mater. Sci.* **17** 2657 (1982)
93. V T Golovchan *Int. J. Refract. Met. Hard Mater.* **28** 250 (2010)
94. W Voigt *Lehrbuch der Kristallphysik* (Leipzig, Teubner, 1928)
95. A Reuss *Angew Z. Math. Mech.* **9** 49 (1929)
96. R Hill *Proc. Phys. Soc. London, A* **65** 349 (1952)
97. S F Pugh *Philos. Mag.* **45** 833 (1954)
98. T Sahraoui, A Kellou, H I Faraoun, N Fenineche, H Aourag, C Coddet *Mater. Sci. Eng. B* **107** 1 (2004)
99. D J Siegel, G Hector, J B Adams *Surf. Sci.* **498** 321 (2002)
100. G M Amulene, M H Manghnani, S Marriappan, X Hong, F Li, X Qin, H P Liermann *J. Appl. Phys.* **103** 113522 (2008)
101. Y A Chang, L E Toth, Y S Tyan *Metall. Trans.* **2** 315 (1971)

102. H L Brown, P E Armstrong, C P Kempter *J. Chem. Phys.* **45** 547 (1966)
103. J A M Ferreira, M A Pina Amaral, F V Antunes, J D M Costa *Int. J. Refract. Met. Hard Mater.* **27** 1 (2009)
104. *CRC Materials Science and Engineering Handbook* (Eds J F Schakelford, W Alexander) (NewYork: CRC Press, 2001)
105. J Haines, J M Leger, G Bocquillon *Annu. Rev. Mater. Res.* **31** 1 (2001)
106. S Veprek, M Haussmann, S Reiprich, L Shizhi, J Dian *Surf. Coat. Technol.* **86** 394 (1996)
107. M H Tsai, S C Sun, H T Chiu, S H Chuang *Appl. Phys. Lett.* **68** 1412 (1996)
108. D J Li, M X Wang, J J Zhang, J Yang *J. Vac. Sci. Technol.* **24** 966 (2006)
109. M X Wang, J J Zhang, J Yang, L Q Wang, D J Li *Surf. Coat. Technol.* **201** 6800 (2007)
110. S H Mohamed *Surf. Coat. Technol.* **202** 2169 (2008)
111. B H Lee, K Yong *J. Vac. Sci. Technol.* **22** 2375 (2004)
112. A V Kuchuk, V P Kladko, V F Machulin, A Piotrowska, E Kaminska, K Golaszewska, R Ratajczak, R Minikayev *Rev. Adv. Mater. Sci.* **8** 22 (2004)
113. S Guruvenket, G M Rao *Mater. Sci. Eng. B* **106** 172 (2004)
114. T Yamamoto, M Kawate, H Hasegawa, T Suzuki *Surf. Coat. Technol.* **193** 372 (2005)
115. M K Neylon, S K Bej, C A Bennett, L T Thompson *Appl. Catal., A* **232** 13 (2002)
116. R McGee, S K Bej, L T Thompson *Appl. Catal., A* **284** 139 (2005)
117. J D Houmes, S Deo, H C zur Loye *J. Solid State Chem.* **131** 274 (1997)
118. S Jeon, K J Yong *Nanotechnology* **18** 245602 (2007)
119. V I Khitrova *Sov. Phys. Crystallogr.* **6** 549 (1962)
120. V I Khitrova, Z G Pinsker *Sov. Phys. Crystallogr.* **6** 882 (1962)
121. D V Suetin, I R Shein, A L Ivanovskii *Zh. Strukt. Khim.* **51** 213 (2010) [a]
122. N N Matyushenko *Kristallicheskie Struktury Dvoinykh Soedinenii* (Crystal Structures of Binary Compounds) (Moscow: Metallurgiya, 1969)
123. J C Grossman, A Mizel, M Cote, M L Cohen, S G Louie *Phys. Rev. B* **60** 6343 (1999)
124. H-T Chiu, S-H Chuang *J. Mater. Res.* **8** 1353 (1993)
125. Z Wu, X-J Chen, V V Struzhkin, R E Cohen *Phys. Rev. B* **71** 214103 (2005)
126. Y Benhai, W Chunlei, S Xuanyu, S Qiuju, C Dong *J. Alloys Compd.* **487** 556 (2009)
127. J Zhou, Z Sun, R Ahuja *J. Alloys Compd.* **472** 425 (2009)
128. L Song, Y X Wang *Phys. Status Solidi B* **247** 54 (2010)
129. A Simunek *Phys. Rev. B* **75** 172108 (2007)
130. N Asada *J. Jpn. Soc. Powder — Powder Metall.* **47** 496 (2000)
131. G Gogova, K Gesheva, A Veneva *Mater. Lett.* **35** 351 (1998)
132. J Jung, S Kang *Acta Mater.* **56** 1379 (2004)
133. Y Li, N Liu, X Zhang, C Rong *Int. J. Refract. Met. Hard Mater.* **26** 33 (2008)
134. D V Suetin, I R Shein, A L Ivanovskii *Zh. Strukt. Khim.* **50** 7 (2009) [a]
135. Z Qiao, X Ma, W Zhao, H Tang, S Cai, B Zhao *J. Alloys Compd.* **456** 514 (2008)
136. J Emmerlich, D Music, A Houben, R Dronkowski, J M Schneider *Phys. Rev. B* **76** 224111 (2007)
137. J Schneider, Z Sun, D Music *J. Phys.: Condens. Matter* **17** 6047 (2005)
138. A L Ivanovskii *Usp. Khim.* **65** 499 (1996) [*Russ. Chem. Rev.* **65** 461 (1996)]
139. N I Medvedeva, D L Novikov, A L Ivanovskii, M V Kuznetsov, A J Freeman *Phys. Rev. B* **58** 16042 (1998)
140. N I Medvedeva, A L Ivanovskii *Zh. Neorg. Khim.* **43** 462 (1998) [h]
141. M W Barsoum, in *Encyclopedia of Materials: Science and Technology* (Amsterdam: Elsevier, 2006) p. 1
142. I R Shein, A L Ivanovskii *Fiz. Tv. Tela* **51** 1517 (2009) [e]
143. D V Suetin, I R Shein, A L Ivanovskii *Physica B* **403** 2654 (2008)
144. D V Suetin, I R Shein, A L Ivanovskii *Zh. Neorg. Khim.* **54** 1503 (2009) [h]
145. D V Suetin, I R Shein, V G Bamburov, A L Ivanovskii *Dokl. Akad. Nauk* **424** 214 (2009) [c]
146. Z Sun, D Music, R Ahuja, S Li, J M Schneider *Phys. Rev. B* **70** 092102 (2004)
147. D Music, Z Sun, R Ahuja, S Li, J M Schneider *Phys. Rev. B* **73** 134117 (2006)
148. H W Hugosson, H Engqvist *Int. J. Refract. Met. Hard Mater.* **21** 55 (2003)
149. M Omori, T Kakita, A Okubo, T Hirai *J. Jpn. Inst. Met.* **62** 986 (1998)
150. D V Suetin, I R Shein, A L Ivanovskii *Physica B* **404** 1887 (2009)
151. K S Aleksandrov, B V Beznosikov *Perovskity: Nastoyashchee i Budushchee* (Perovskites: The Present and the Future) (Novosibirsk: Siberian Branch of the Russian Academy of Sciences, 2004)
152. P S Herle, M S Hegde, K Sooryanarayana, T N Guru Rowa, G N Subbanna *J. Mater. Chem.* **8** 1435 (1998)
153. D V Suetin, V V Bannikov, I R Shein, A L Ivanovskii *Phys. Status Solidi B* **246** 1646 (2009)
154. R A Johnson *Phys. Rev. B* **37** 3924 (1988)
155. I R Shein, A L Ivanovskii *Mater. Lett.* **63** 2413 (2009)
156. A R Trueman, D P Schweinsberg, G A Hope *Corros. Sci.* **41** 1377 (1999)
157. L G Yu, K A Khor, H Li, K C Pay, T P Yip, P Cheang *Surf. Coat. Technol.* **182** 308 (2004)
158. H Li, K A Khor, L G Yu, P Cheang *Surf. Coat. Technol.* **194** 96 (2005)
159. X Q You, S Zhang, X F Song, M P Huang, J G Ma *Appl. Surf. Sci.* **253** 4409 (2007)
160. Y Q Fu, F Zhou, Y Gao, L Z Zhang *Rare Met. Mater. Eng.* **36** 731 (2007)
161. X Q You, C J Zhang, N Liu, M P Huang, J G Ma *J. Mater. Sci.* **43** 2929 (2008)
162. O O Eso, P Fan, Z Z Fang *Int. J. Refract. Met. Hard Mater.* **26** 91 (2008)
163. Z H Wang, A D Yang, D Y He, J M Jiang *Rare Met. Mater. Eng.* **37** 1869 (2008)
164. A Bedolla-Jacuinde, R Correa, I Mejia, J G Quezada, W M Rainforth *Wear* **263** 808 (2007)
165. X Zhi, J Xing, Y Gao, H Fu, J Peng, B Xiao *Mater. Sci. Eng. A* **487** 171 (2008)
166. G Pintaude, F G Bernardes, M M Santos, A Sinatora, E Albertin *Wear* **267** 19 (2009)
167. Z Liu, Y Li, X Chen, K Hu *Mater. Sci. Eng. A* **486** 112 (2008)
168. T Tsuchida, N Morita *J. Eur. Ceram. Soc.* **22** 2401 (2002)
169. T Tsuchida, K Suzuki, H Naganuma *Solid State Ionics* **141–142** 623 (2001)
170. W B Mercado, J Cuevas, I Y Castro, M Fajardo, G A P Alcazar, H S Sthepa *Hyperfine Interact.* **175** 49 (2007)
171. R Subramanian, J H Schneibel *Intermetallics* **5** 401 (1997)
172. R Subramanian, J H Schneibel *Mater. Sci. Eng. A* **244** 103 (1998)
173. J Voyer, R B Marple *Wear* **225–229** 135 (1999)
174. A Bellosi, V Medri, F Monteverde *J. Am. Chem. Soc.* **84** 2669 (2001)
175. N A Dubrovinskaia, L S Dubrovinsky, S K Saxena, M Selleby, B Sundman *J. Alloys Compd.* **285** 242 (1999)
176. V Ramnath, N Jayaraman *J. Mater. Sci. Lett.* **6** 1414 (1987)
177. S Yang, S Andersson *Acta Crystallogr., Sect. B* **43** 1 (1987)
178. J Leciejewicz *J. Less-Common Met.* **7** 318 (1964)
179. A V Ilyasov, A A Ryzhkin, V V Ilyasov *Zh. Strukt. Khim.* **49** 827 (2008) [a]
180. D V Suetin, I R Shein, A L Ivanovskii *Physica B* **404** 3544 (2009)
181. Y Li, Y Gao, Z Fan, B Xiao, Q Yue, T Min, S Ma *Physica B* **405** 1011 (2010)
182. B C Muddle *Metall. Trans. A* **15** 1089 (1984)
183. M Christensen, S Dudiy, G Wahnstrom *Phys. Rev. B* **65** 045408 (2002)
184. M Christensen, G Wahnstrom *Phys. Rev. B* **67** 115415 (2003)

185. A A Knizhnik, A A Safonov, I M Iskandarova, A A Bagatur'yants, B V Potapkin, L R C Fonseca, M W Stoker *J. Appl. Phys.* **99** 084104 (2006)
186. A Varykhalov, O Rader, W Gudat *Phys. Rev. B* **72** 115440 (2005)

[a] — *J. Struct. Chem. (Engl. Transl.)*
[b] — *Theor. Exp. Chem. (Engl. Transl.)*
[c] — *Dokl. Phys. Chem. (Engl. Transl.)*
[d] — *J. Exp. Theor. Phys. Lett. (Engl. Transl.)*
[e] — *Phys. Solid State (Engl. Transl.)*
[f] — *Inorg. Mater. (Engl. Transl.)*
[g] — *Tech. Phys. Lett. (Engl. Transl.)*
[h] — *Russ. J. Inorg. Chem. (Engl. Transl.)*